

University of Nebraska - Lincoln

DigitalCommons@University of Nebraska - Lincoln

Industrial and Management Systems
Engineering -- Dissertations and Student
Research

Industrial and Management Systems
Engineering

Fall 12-5-2013

MODELLING OF ANODE CRATER FORMATION IN MICRO-ELECTRICAL DISCHARGE MACHINING

Avinash Deshmukh

University of Nebraska-Lincoln, deshmukh.avi@gmail.com

Follow this and additional works at: <https://digitalcommons.unl.edu/imsediss>

Deshmukh, Avinash, "MODELLING OF ANODE CRATER FORMATION IN MICRO-ELECTRICAL DISCHARGE MACHINING" (2013). *Industrial and Management Systems Engineering -- Dissertations and Student Research*. 41.

<https://digitalcommons.unl.edu/imsediss/41>

This Article is brought to you for free and open access by the Industrial and Management Systems Engineering at DigitalCommons@University of Nebraska - Lincoln. It has been accepted for inclusion in Industrial and Management Systems Engineering -- Dissertations and Student Research by an authorized administrator of DigitalCommons@University of Nebraska - Lincoln.

MODELLING OF ANODE CRATER FORMATION IN MICRO-ELECTRICAL
DISCHARGE MACHINING

by

Avinash Deshmukh

A THESIS

Presented to the Faculty of

The Graduate College at the University of Nebraska

In Partial Fulfillment of Requirements

For the degree of Master of Science

Major: Industrial and Management Systems Engineering

Under the Supervision of Professor Kamlakar P.Rajurkar

Lincoln, Nebraska

December, 2013

MODELLING OF ANODE CRATER FORMATION IN MICRO-ELECTRICAL DISCHARGE MACHINING

Avinash Deshmukh, M.S.

University of Nebraska, 2013

Adviser : Kamlakar P. Rajurkar

With rapid technology development in the fields of biomedical devices, aerospace, automobile, energy, semiconductors, biotechnology, electronics and communication, the use of micro parts and devices with micro-features has become indispensable. Micro-Electrical Discharge Machining (micro-EDM) because of its inherent characteristics is capable of fabrication of three-dimensional complex micro components and microstructures. However, due to difficulty in fully understanding of material removal mechanism, limited knowledge of process characteristics, lower material removal rate compared with other micromachining technique, the micro-EDM is only used in niche application. Therefore, in order to fully utilize the potential of micro-EDM, focused studies are needed to understand the fundamentals of process mechanism through crater formation, tool wear, debris formation, relationship between process parameter and process performance measures.

The aim of this research work is to develop a predictive thermal model for the simulation of single-spark micro-EDM at anode surface. Finite Element Analysis was performed to solve this model using commercial available software COMSOL. This model assumed a Gaussian distribution heat flux, constant heat flux radius, constant fraction of total energy transferred to anode, temperature dependent material properties to perform transient thermal analysis to predict single discharge crater geometry and temperature distribution

on the workpiece for different discharge energy levels (less than $1\mu\text{J}$). The simulated part whose temperature was higher than melting temperature considered as removed part. The experiments were performed for single discharge spark using a Resistor-Capacitor (RC) with titanium alloy Ti-6Al-4V (Grade 5) as workpiece material and tungsten as tool electrode. The experimental crater dimensions were measured by using atomic force microscope (AFM). The simulated craters dimensions were compared with experimental craters. Results showed close agreement between simulated crater radii and experimental crater radii for the discharge energy range up to $1\mu\text{J}$.

ACKNOWLEDGEMENTS

I would like to express my gratitude to my adviser, Dr. Rajurkar, for his continuous guidance and support during the length of my Master's study here at the University of Nebraska, Lincoln. I would like to thank him for giving opportunity to work at Center for Non-traditional Manufacturing Research (CNMR). His commitment to quality research, attention to every detail and discipline has been a constant source of motivation for me.

I would like to thank Dr. David Olson and Dr. Ram Bishu for consenting to serve on my thesis committee. Their willingness to serve on the committee, valuable comments and insights are greatly appreciated.

I wish to thank my mentor at the CNMR, Dr. Lin Gu for his constant support and valuable inputs during the process of this thesis. I would like to thank my friend Bai Shao for his extended help with Scanning Electron Microscope

I thank my friends and colleagues at CNMR for making my stay in Lincoln enjoyable and a very good learning experience.

I express my gratitude towards my parents for their love and constant encouragement. They had a great influence on my academic choices and career path. Finally I dedicate this thesis to my late grandfather who was always very encouraging and supportive of my graduate education.

TABLE OF CONTENTS

CHAPTER 1. INTRODUCTION	1
1.1 Background	1
1.1 ELECTRICAL DISCHARGE MACHINING (EDM)	2
1.1.1 MICRO-ELECTRO DISCHARGE MACHINING (micro-EDM)	4
1.2 PURPOSE OF RESEARCH	5
1.3 Thesis Organization	6
Chapter 2. LITERATURE REVIEW	7
2.1 Basics of EDM	7
2.1.1 Evolution of EDM Process	7
2.1.2 Theory of EDM Process	11
2.1.3 Comparison of Conventional (macro) EDM and micro-EDM	25
2.2 Process modelling in EDM and micro-EDM	27
2.3 Conclusion of Literature Review	35
Chapter 3. EXPERIMENTAL METHODS AND MEASUREMENT TECHNIQUES FOR SINGLE SPARK ANALYSIS	35
3.1 EXPERIMENTAL OBJECTIVES	35
3.2 Experimental setup	36
3.2.1 Micro-EDM MACHINE	36
3.2.3 Work piece and tool electrode	39
3.3 Work piece preparation	40
3.4 Characterization techniques	40
3.4.1 Voltage and current probes with oscilloscope	40
Chapter 4. PROCESS MODELLING AND SIMULATION	44
4.1 Single electrical discharge model for micro-EDM	44

4.2 Modelling with finite element method	44
4.2.1 Physical description	45
4.2.2 Thermal conduction model	48
4.3 Numerical model	52
4.4 Simulation Results and discussion	54
4.4.1 Temperature distribution	55
Chapter 5. EXPERIMENTS	64
5.1 Single Spark experiment	64
5.2 Experiment Design	65
5.3 Experiment Results and Discussion	67
5.3.1 Measurement of Process Parameters	68
5.3.2 Effect of discharge Energy on crater Geometry	77
5.3.3 Effect of Pulse on time on crater geometry	78
Chapter 6. CONCLUSIONS AND RECOMMENTATIONS	81
6.1 Conclusions	81
6.2 Recommendations for future work	82
REFERENCES	83

LIST OF FIGURES

Figure 1 Basic schematic of an EDM system	3
Figure 2.1 Electro thermal material removal mechanism	14
Figure 3.1 Micro-EDM machine	417
Figure 3.2 RC Pulse generator for micro-EDM	38
Figure 3.3 Typical voltage and current waveforms	41
Figure 4.1 Schematic sketch of the physical model	47
Figure 4.2 2D Model for micro-EDM process	47
Figure 4.3 Mesh generation for FEM full model	62
Figure 4.4 Temperature variation with respect to distance for discharge condition I (0.1 μJ)	56
Figure 4.5 Temperature variation with respect to distance for discharge condition II (0.238 μJ)	57
Figure 4.6 Temperature variation with respect to distance for discharge condition III (0.273 μJ)	58
Figure 4.7 Temperature variation with respect to distance for discharge condition IV (0.373 μJ)	59
Figure 4.8 Temperature variation with respect to distance for discharge condition V (0.6 μJ)	60
Figure 4.9 Temperature variation with respect to distance for discharge condition VI (1.087 μJ)	61
Figure 4.10 Thermal distribution for heat flux on a workpiece	63
Figure 5.1 Discharge craters generated during discharge condition I	75
Figure 5.2 Waveform at various discharge conditions	69
Figure 5.3 Experimental crater formed under Discharge condition I (0.1 μJ)	71
Figure 5.4 Experimental crater formed under Discharge condition II (0.238 μJ)	72
Figure 5.5 Experimental crater formed under Discharge condition III (0.273 μJ)	73

Figure 5.6 Experimental crater formed under Discharge condition IV (0.373 μJ)	74
Figure 5.7 Experimental crater formed under Discharge condition V (0.6 μJ)	75
Figure 5.8 Experimental crater formed under Discharge condition VI (1.087 μJ)	76
Figure 5.9 Effect of measured discharge energy on crater diameter	77
Figure 5.10 Effect of measured discharge energy on crater depth	78
Figure 5.11 Effect of Pulse on time on Crater Diameter	78
Figure 5.12 Effect of Pulse on time on Crater Depth	79
Figure 5.13 Comparison of predicted and experimental crater geometries	80

LIST OF TABLES

Table 2.1 Process parameters effects on machining condition	17
Table 2.2 performance measures that are used to determine process performance results	21
Table 2.3 Comparison between micro-EDM and conventional EDM [9]	26
Table 3.1 Chemical composition of titanium material	39
Table 3.2 Thermo-physical properties of titanium material	39
Table 5.1 Experimental parameters for single spark experiment	65
Table 5.2 Input parameters for each experimental run	66
Table 5.3 Parameter measured from voltage and current waveform	68

CHAPTER 1

INTRODUCTION

1.1 Background

With rapid technology development in the fields of biomedical devices, aerospace, automobile, energy, semiconductors, biotechnology, electronics and communication, the use of micro parts and devices with micro-features has become indispensable. The Microsystems-based products such as medical implants, drug delivery system, diagnostic devices, connectors, switches, micro-reactors, micro-engines, micro-pumps and printing heads, represents key value-adding elements for many companies and thus, an important contributor to a sustainable economy [1]. In order to meet the increasing demand of manufacturing micro products and components in terms of tighter tolerances, higher accuracy and precision, superior surface integrity, improved reliability and repeatability, the capabilities of micro-manufacturing processes have to be continuously enhanced. Therefore, the continuous research to improve existing micro-machining techniques is essential to meet future micro-manufacturing needs.

The advent of photolithography on silicon substrate has not only revolutionized micro electro-mechanical systems (MEMS) technologies but also it has established MEMS as an earliest competitive micro-machining process [2]. However, MEMS based techniques have limitations such as inability to fabricate miniaturized products and components that require complex three dimensional and high aspect ratio features, limited selection of work materials (mostly silicon based) , huge capital cost and restrictive clean environment [3, 4]

To meet these limitations of MEMS-based machining processes, traditional machining processes such as drilling, grinding, milling and turning have been evolved in micro-machining application over the period of time, where tool comes in direct mechanical contact with workpiece [4, 5]. These processes are capable of not only drilling micromoles, turning cylindrical shapes and fabrication of 2D and 3D micro-features but also have high material removal rate. However these traditional machining processes have limitations such as inability to machine advance material with high hardness, fabrication of micro-parts with complex geometries, lower rigidity and incapable for mass production. To address these limitations of traditional machining processes, non-traditional machining processes are emerged as alternative techniques for micro-machining[6]. Typical non-traditional machining processes are laser beam machining (LBM), focused ion beam machining (FIBM), ultrasonic machining (USM) and electrical discharge machining (EDM).

1.1 ELECTRICAL DISCHARGE MACHINING (EDM)

EDM is a thermo electric process which removes material from electrically conductive workpiece using series of discrete sparks that occurring between tool and workpiece in presence of dielectric fluid. The schematic illustration of EDM is shown in Fig. 1. where both tool and workpiece are immersed in and separated by certain distance in a tank that filled with dielectric fluid.

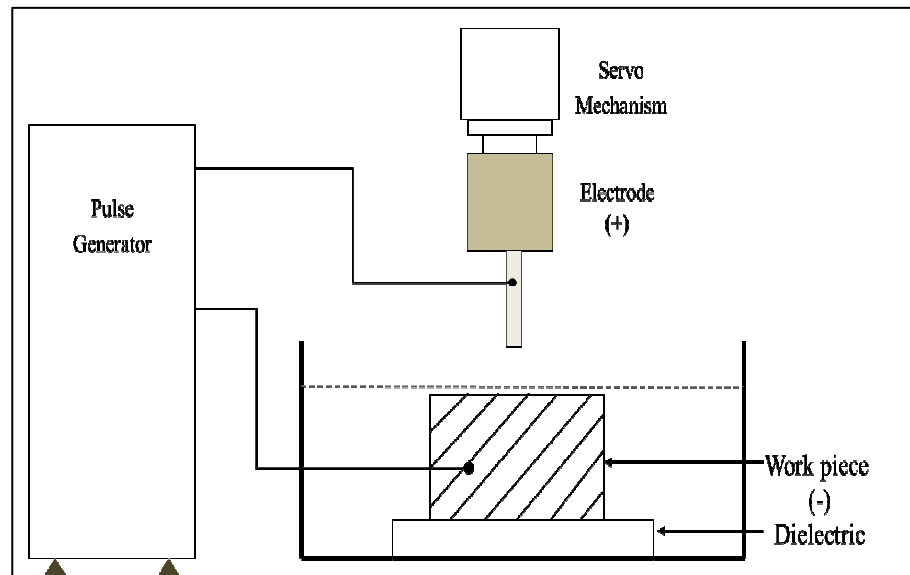


Figure 1 Basic schematic of an EDM system

The tool moves downward towards the workpiece until gap between tool and workpiece reaches critical value (called as spark gap) so that applied voltage is high enough to breakdown dielectric and spark discharge takes place between tool and workpiece. During the discharging process, electrical energy from a pulse generator is turned in to thermal energy which generates a channel of plasma in the working gap between tool and workpiece at a very high temperature. This high temperature removes material from workpiece as well as tool by melting and vaporization. The melted material is removed in the form of debris by flowing dielectric fluid

EDM has the following major advantages over the traditional machining process.

- Capable to machine any conductive material regardless of its hardness

- Absence of mechanical contact between the tool and workpiece which eliminates mechanical deformation problems
- The edges of parts machined are burr free
- Capable to machine complex 3D structures
- No pollution or filings that require expensive cleaning procedures

These unique features make EDM a very versatile process in the manufacturing of complex shaped dies and molds of high strength materials. However, EDM can machine only electrically conductive materials.

1.1.1 MICRO-ELECTRO DISCHARGE MACHINING (micro-EDM)

The downscaling of electrodischarge machining for machining micro parts and micro features with high accuracy is termed as micro-electrodischarge machining (micro-EDM). In micro-EDM the discharge energy between tool and workpiece is minimized and discharge current with an extremely short pulse width is used. In Micro-EDM- the principle of material removal is same as the conventional EDM i.e. by electro-thermal erosion phenomenon (absence of mechanical contact between tool and workpiece during material removal process). Micro-EDM because of its unique features such as absence of physical contact and significant forces between tool and workpiece enables to use tools with finer form and lower rigidity for machining and fabrication of intricate parts without significant tool and workpiece deflection. Also, micro-EDM requires simple equipment set up and low capital equipment cost. Micro-EDM because of its ease of implementation

stands out as most widely adopted nontraditional machining technique, outselling all other processes excluding milling, turning and grinding [7].

1.2 PURPOSE OF RESEARCH

Micro-EDM is used in various specialized processes like fabrication of high aspect ratio micro-holes in inject nozzles and fuel injection nozzles as well as in manufacturing of dies and moulds for mass production of micro-parts [8]. Although micro-EDM has already carved a niche itself as reliable micro manufacturing technique with its development, there are some process shortcomings such as lower material removal rate as compared to other micro-machining techniques, difficulties in understanding material removing mechanism and the effects of process parameters on performance measures, stochastic nature of process and occurrence of tool wear which limit its ability to attain wider range of utilization [9]. Therefore recent research has been concentrated on improving micro-EDM machining performance, such as Material Removal Rate, Tool Wear Rate and surface roughness. Although many studies have been conducted to address these areas, the outcome in terms of material removal mechanism and process characteristics are not clearly understood yet. Therefore, new process modelling and simulation approach is essential in order to fully utilize the capability of micro-EDM in wide range of application.

In this study, thermal electrical theoretical model for a single discharge micro-EDM has been developed to determine crater geometry at anode at different energy level. Finite element method based commercially available software COMSOL is used to solve the underlying governing equation and associated model-specific boundary conditions. The simulation results were compared with experimental results.

The objectives of this research work are given below.

1. Conduct an experimental study to identify the relationship between discharge energy (less than $1\mu\text{J}$) and crater geometry of micro-EDM.
2. Perform Finite Element Method (FEM) to predict crater geometry and temperature distribution on the workpiece for micro-EDM.
3. To validate the simulation results with experimental results.

1.3 Thesis Organization

Chapter 2 covered critical literature review. This literature will cover basics of EDM and process modelling in EDM and Micro-EDM

Chapter 3 includes the experimental methodology and measurement techniques used for single spark crater..

Chapter 4 presents the development of theoretical model for single discharge in micro-EDM.

Chapter 5 presents experimental results of single spark. The effect of process parameters on crater geometry is discussed. Model results were compared with experimental results.

Chapter 6 presents the conclusions and future work.

CHAPTER 2

LITERATURE REVIEW

This chapter present literature review of electrical discharge machining (EDM) as a technique for micro machining. This chapter is divided into three sections: 1. Basics of EDM, 2. Review of process modelling in EDM and micro-EDM and 3. Conclusion of literature review. The basics of EDM will provide the evolution of EDM, theory of EDM process and a comparison between EDM and micro-EDM.

2.1 Basics of EDM

The basics of EDM are first presented in the literature review prior to a critical literature review on process modelling of EDM and micro-EDM. This section presents a brief history of EDM and theory of EDM process in order to understand the EDM process. Finally, the last part describes distinction between EDM and micro-EDM. While covering EDM process theory, the material removal mechanism by electro-thermal nature, EDM process parameters and process performance are described.

2.1.1 Evolution of EDM Process

The origin of EDM can be traced as far as in 1770 when English chemist Joseph Priestly firstly detected the erosive effect of electrical discharge machining on metals [10]. However, due to the same volume of the workpiece and electrode material removal during the process, it was difficult to utilize this process efficiently. In 1943, the Russian scientists Boris Lazerenko and Natalya Lazerenko carried out revolutionary work on

Electrical Discharge Machining at Moscow University[10]. The Lazerenkos developed a spark machining process by analyzing the destructive properties of electrical discharge. The Lazerenko EDM system used resistance-capacitance (RC) power supply, which became the model for future RC-type pulse generating systems in use for EDM technology.

The pulse generating system is one of the key elements in EDM which provides energy across the discharge gap to remove material. It directly affects the machining speed, machining precision, machining stability, surface roughness of workpiece and tool wear ratio in EDM [11]. The most commercially used pulse generators in EDM are Resistance-Capacitance (RC) type and Transistor-type pulse generators. RC- type generators provide small discharge energies with very short pulse on time interval of sub-microsecond range therefore they are used in finishing and micro-machining [12]. Transistor-type generators are capable of generating higher frequency isopulses, i.e., repeated pulses with identical duration and magnitude; therefore they are employed in production of machined surfaces with controlled finishes [13, 14]. Although developed transistor-type isopulse generators are suitable for micromachining through evaluation of machining characteristic, RC-type pulse generators are still commonly used due to its simplicity of design.

In order to use EDM as reliable machining technique while making consistent efforts in obtaining continuous machining performance outcomes and achieve accurate control of machining process, it is necessary to explore ways of process planning by process characteristics knowledge. Thus, extensive research and development effort have been directed in establishing EDM process characteristics, optimizing process parameters

based on process analysis[15, 16], advance process modelling [17-19], monitoring, control and automation [20, 21].

The increase in popularity of EDM in manufacturing world caused the shift from basic research to a more pragmatic, applied research [22]. Therefore, much research interest has focused in new EDM technique such as micro-machining [23, 24], machining of insulating ceramic materials [25, 26], powder mixed dielectric EDM machining [27, 28], hybrid processes by combining EDM with other machining [29, 30], dry EDM [31-34] and near dry EDM [35].

2.1.1.1 Application of Micro-EDM in micro-machining

The downscaling of EDM to micro level in micromachining application is defined as Micro-EDM. The unique features of Micro-EDM which makes its one of the most powerful micro-machining technique in comparison with other micro machining techniques are highlighted as follows.

- Suitable for machining any electrically conductive and semi-conductive material
- Absence of mechanical contact between tool electrode and workpiece
- Negligible contact forces induced between tool electrode and workpiece
- Capable to machine high aspect ratio features
- Capable to machine three dimensional features
- Capable to machine complex features in single workpiece setting
- Capable to machine with minimal formation of burrs at machined edges

- A relatively versatile, reliable and cost effective machining method

The unique feature which makes Micro-EDM as one of the important process in micromachining is its ability to machine any material with electrical resistivity up to 100 Ωcm [36], with high surface accuracy regardless of its hardness and without additional workpiece conditioning [37]. As there is no physical contact between tool electrode and workpiece, the machining forces are very low during the machining. This enables to use thin tools for machining complex features with minimal tool and workpiece deflection. Micro-EDM is capable of not only drilling micro holes with high aspect ratio and blind non circular holes with sharp corners and edges [38] but also milling three-dimensional profiles without repositioning workpiece to ensure minimal positioning errors [39]. Micro EDM allows obtaining high quality in shape and texture of machined surface with minimum burrs [40] or without burrs [41] which reduces manufacturing time in terms of performing deburring processes and avoid damage of micro-features. Due to simple equipment set up and low capital cost, Micro EDM becomes cost effective, reliable and versatile micro machining technique.

In a review of developments in three dimensional micro machining using machine tools, it was proposed that Micro-EDM is the most effective technique for machining concave shapes due to the negligible machining forces and the ease of incorporating tool making subsystem such as wire electro discharge grinder (WEDG) on the Micro-EDM machine [42]. Moreover, It was indicated that Micro-EDM can be extensively adopted in EDM application [10]. Micro-EDM has been successfully tested for fabrication of micro-holes on insulating ceramics using assisted electrode method similar to EDM [43]. In addition, Micro-EDM has demonstrated its versatility in complex three dimensional structuring of

silicon through fabrication of various features which were proved to be difficult using MEMS based etching process [44]. Furthermore, Micro-EDM have been used in developing hybrid micro-machining process (HMP) in which Micro-EDM is combined with other material removing process such as laser machining to exploit synergism of these processes in terms of improving material removal or facilitating better machining conditions[45]. Based on the feasibility of applying EDM as alternative micro machining technique, Micro-EDM process has been developed over wide range of mode of applications such as die-sinking [46], drilling [47], milling [48], wire cutting [49], wire grinding [23] and turning [50]. However, the true potential of these processes measured in terms of their commercial applications are still limited to niche areas such as spinneret holes for synthetic fibers, production of tapered holes for diesel fuel injection nozzles, drilling of high aspect ratio micro-holes for inject-nozzles and micro-moulds making for mass replication processes [8]. To further enhance Micro-EDM technology's competitiveness as alternative micro-machining technique and to meet the growing demand of miniaturized, precision parts in different industry application, it is necessary to improve machining performance of the Micro-EDM process by understanding EDM process characteristics.

2.1.2 Theory of EDM Process

Almost about 70 years passed since the discovery of EDM technology, the exact physical phenomenon taking place during material removal in EDM is not yet fully understood [51]. The various theories based on theoretical and experimental research have been proposed to address the material removal mechanism of the EDM process. These theories

can be broadly categorized into two modes such as “electro-thermal mechanism” and “electro-mechanical mechanism” [52].

Electro-thermal Mechanism – It is suggested that thermal melting and superheating are the dominant mechanism for the electrode material removal due to heat transfer from a superheated and highly pressurized plasma channel formed between the electrodes during an electrical discharge [53].

Electro-mechanical Mechanism – It is suggested that “yielding” is the main mechanism for electrode material removal for short pulses (discharge duration $<5\mu\text{s}$) due to stresses generated within electrode by electrostatic forces acting on the electrode surface such that regions subjected to higher stresses than material yield strength [54].

Out of these two modes, electro-thermal mechanism is the most widely accepted process mechanism, which is discussed more in detail in the following section.

2.1.1.2 The electro-thermal mode of material removal

The electro thermal material removal mechanism composed of three stages namely, pre-discharge phase, discharge phase and post-discharge phase. The following phases shown in figure 2.1 illustrate electro thermal material removal mechanism.

b) In a typical EDM process, the electric discharge occurs in between positively-charged anode and negatively charged cathode in presence of a dielectric medium. When electric voltage input is applied across the cathode and anode, cathode emits the electrons.

c) The electrons emitted from cathode collide with neutral atoms and particles in presence of dielectric medium along their path in between cathode and anode. This

results in formation of more electrons and ions. However, in some cases the conducting particles, such as debris of previous discharges are concentrated and attracted to areas with high electrical field intensity. The accumulation of particles aids in creating a bridging effect which reduces the inter-electrode gap and helps in discharge initiation.

d) Due to the difference between mass of newly formed electrons and ions, newly formed electrons move at faster speed towards the anode as compared to ions which move towards the cathode. During this process electrons get accelerated, more electrons and ions would get generated due to the collision with more neutral atoms and particles. This cyclic process resulting in avalanche like formation of electrons and ions is known as impact ionisation. After the abridgment of inter-electrode gap by electrons, the dielectric breakdown occurs and discharge phase begins.

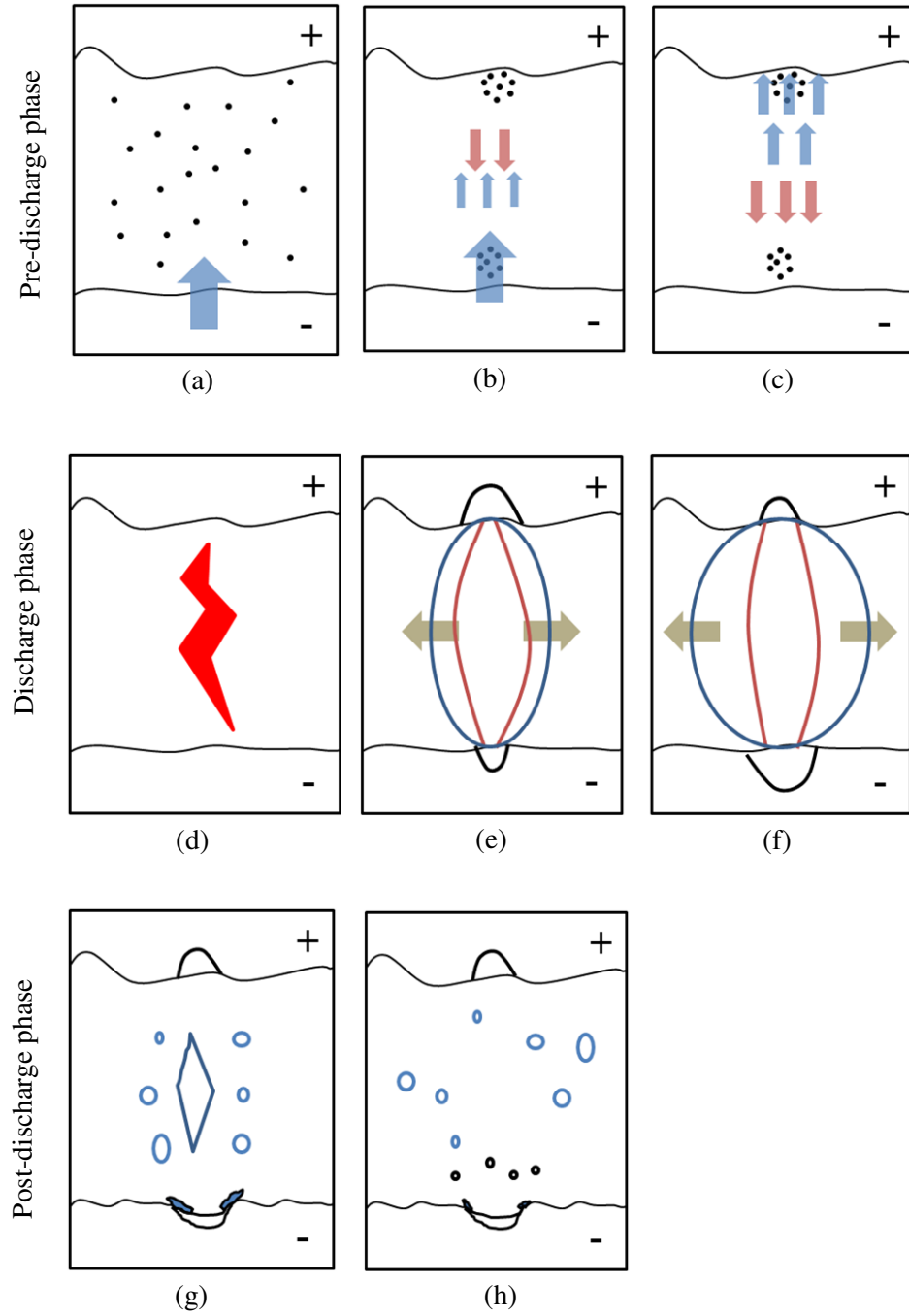


Figure 2.1 Electro thermal material removal mechanism

e) After breakdown, resulting conductive channel aids in easy movement of emitted electrons from cathode towards anode and intensifies the impact ionisation. This impact ionisation leads to formation of a plasma channel which generates a high heat flux because of its high current density. This plasma channel causes melting of electrodes. The temperature of plasma channel has been measured experimentally using the spectroscopy. It was reported that plasma channel temperature range from 4000K to 8000K [55, 56] and 8000K to 10000K [56].

f) The plasma channel continues to expand rapidly with continued emission of electron from cathode. During this phase, the high temperature from plasma vaporizes, disassociates and ionizes the dielectric at interface of plasma channel and dielectric, causing the formation and rapid expansion of a gas bubble [53]. The pressure within bubble becomes very high due to the inertia and viscosity of dielectric and the boundary between bubble and dielectric expands with the several tens m/s [12]. It was reported that pressure builds within bubble range between 6bars and 14 bars [57]. This bubble pressure plays a significant role in superheating molten material with minimal vaporization [58] which results in formation of a pool of molten material, called as a melt pool. Some of the molten material gets pushed out from the melt pool due to pressure within bubble. It was suggested that the anode melts first before cathode because the electrons in the plasma channel move faster than ions and therefore a larger melt pool formed at the anode during the initial stages of discharge [59]. As the discharge durations in micro-EDM are in sub-microsecond range, the workpiece is set as anode and tool electrode set as cathode so that material removal is greater than tool wear.

g) Heat flux density afterward decreases at the anode with further expansion of plasma channel. It supports re-solidification of molten material as heat is conducted away from the melt pool through base material. However the molten material at cathode increases due to the impact of lower moving speed of positive ions [59]. Similar to the anode, some of the molten material also gets pushed out from the melt pool due to the pressure within bubble. This discharge phase comes to end when the discharge voltage applied across the electrodes is turned off or discharge current stops.

h) When the supplied voltage or discharge current is turned off, the plasma channel collapses and bubble implodes violently and dielectric flushes in. The implosive force due to the sudden drop of pressure causes the molten material in the melt to be partially expelled. As the majority of molten material re-solidifies at the anode before the collapse of plasma channel, there will be minimum expulsion of material occurred.

i) The dielectric cools and solidifies the expelled molten material. The sudden drop in temperature due to dielectric rush retains molten material in melt pool which re-solidifies as recast region of resulting crater.

2.1.2.2 Process Parameters and Performance measures

Process parameters are the controllable input variables that affect the machining condition of the micro-EDM process. These machining conditions determine the process performance result, which are assessed by performance measures. The process parameters and their effects on the machining condition are enlisted in table 2.1. The various performance measures that are used to determine process performance results are presented in table 2.2

Table 2.1 Process parameters effects on machining condition

Process parameter	Effect on machining condition
Pulse on time	Pulse on time is the discharge duration in which material removal takes place. During this time period current flows through cathode towards work material which results in formation of plasma channel causing heating of material. The longer the pulse on time, higher is the single pulse Discharge energy.
Pulse off time	Pulse off time is the time duration between two consecutive pulses on time period. During this time period, there is no discharge takes place between two electrodes as pulse generator is sets off is sets of in zero state. This parameter is important in order to make sure that deionization of dielectric takes place from previous discharge and dielectric regain its insulating properties. The Longer pulse off time

	helps in obtaining stable machining condition by avoiding arcing.
--	---

Process parameter	Effect on machining condition
Pulseoff time	
Voltage	<p>Input voltage applied when the distance between tool electrode and material is too large, is called as open circuit voltage (V_{oc}). As there is no flow of current between tool electrode and material, this parameter do not contribute to any material removal or tool wear.</p> <p>During this condition V_{oc} increases until it creates ionization path through dielectric. Once the dielectric ionization occurs, current starts to flow. As current flows through dielectric, V_{oc} drops to discharge voltage (V_d). Higher V_d settings increases discharge energy and also helps in improving flushing condition by increasing the gap distance.</p> <p>As voltage V_d is not constant during pulse on time, V_d quantified as average discharge voltage (V_{av}).</p>
Current	<p>The discharge current (I_d) is known as the quantity of electrical charges flowing between the tool and workpiece electrode through dielectric medium. This parameter is important in Edm machining</p>

	because it causes primary heating mechanism. The discharge energy increases with increase in I_d . In an RC-type pulse generator, I_d is not constant during pulse on time, I_d quantified as average discharge current (I_{av}) or peak discharge current (I_{pk})
Discharge Gap distance	Discharge Gap distance is the maximum distance between the tool electrode and workpiece material where spark occurs. It is influenced by discharge energy.

Process parameter	Effect on machining condition
Discharge Energy	Input discharge energy (E_{in}), also referred as discharge energy, and is electrical energy used for material removal in discharge machining. In an RC-type pulse generator, this discharge energy is equal to stored energy in capacitor which depends upon applied capacitance and V_{oc} . The amount of discharge is quantified from measured pulse on time, discharge voltage and discharge current.
Dielectric	Dielectric act as medium which allow the controlled spark across the gap between tool electrode and workpiece. Plasma channel growth, force of plasma channel implosion and expulsion of molten material are effected partly by the dielectric medium. Dielectric medium acts as

	<p>quenching medium to cool and solidify the expelled molten material into debris during discharge. It helps in debris flushing by carrying away solidified debris across discharge gap. It also acts as heat transfer medium to absorb and cools the electrode and workpiece by drawing away the heat generated from the discharge locations. The selection of dielectric is crucial in EDM process because the properties of dielectric affect the processes performance with change in machining condition across the spark gap [60, 61].</p>
<p>Electrode Polarity</p>	<p>Polarity of pulse generator connected to tool electrode and workpiece can either be positive or negative depending upon the wear dominance of respective electrode during pulse on time. In general, the polarity of cathode in Micro-EDM is negative so that wear of workpiece dominates.</p>

Process parameter	Effect on machining condition
Flushing	<p>Flushing is the process of removing the debris from the discharge gap and improves surface finish of machined material. It also supply fresh dielectric to the dielectric gap and cools the both electrode and workpiece. The insufficient flushing can results into unstable machining due to the accumulation of debris within the discharge gap.</p>

	<p>It was found that flushing affects MRR and TWR in roughing process, also it affects the SI in finishing process [62]. In order to obtain good flushing condition in the discharge gap for conventional EDM, various methods have been developed such as forced flushing, jet flushing, immersion flushing and modification of tool electrode [63]. However, most of these methods are not suitable for micro-EDM due to the tool electrode and machined feature small size limitation and induced vibration which leads to bending or breakage of tool or feature. In micro-EDM, flushing effects are typically obtained by rotary motion of electrode or the workpiece [50, 64], ultrasonic vibration [65], magnetic field flushing [66] and gravity assisted flushing [67].</p>
--	--

Table 2.2 performance measures that are used to determine process performance results

Performance measure	Process Performance result
Material Removal Rate (MRR)	MRR is considered as primary performance measure which reflects the erosion rate of the workpiece. Beside

	<p>the volumetric amount of workpiece material removal per unit time, the speed at which machining is carried also quantified in MRR measurement. MRR can be expressed as the ratio of volume of material removed from the workpiece to the total machining time.</p>
Tool Wear rate (TWR)	<p>TWR is considered as performance measure which reflects the erosion rate of the tool electrode. Beside the volumetric amount of workpiece material removal per unit time, it also plays an important role in geometrical accuracy of machined feature.</p>
Wear ratio (WR)	<p>WR in micro-EDM is influenced by parameters such as TWR and MRR. WR is expressed as the ratio of TWR/MRR. This parameter is used to quantify tool-workpiece material combination pairs as different material combination leads to different TWR and MRR values. TWR can be improved by using a material combination pair which gives optimal TWR and MRR condition.</p>

Performance measure	Process Performance result
Surface Integrity (SI)	Surface Integrity is a crucial performance measure used to

	<p>describe the inherent or enhanced condition of the machined surface, comprises surface roughness (SR), depth of heat affected zone (HAZ), recast layer thickness and micro crack density.</p>
Surface roughness (SR)	<p>Surface roughness (SR) is a performance measure that expresses the texture of the machined surface. The most commonly used parameters to measure the SR are Ra (arithmetic mean roughness value), Rmax (maximum peak-to-valley height) and Rq (root mean square roughness value). It has been reported that discharge energy influences surface roughness [68, 69].</p>
Recast layer thickness	<p>Recast layer is an uneven, non-etchable topmost surface layered of machined surface which is formed by molten material solidifying at high temperature after discharge process. This layer is often referred as “white layer”. It has been reported that recast layer thickness is more influenced by pulse on time than peak current [68, 69].</p>

Performance measure	Process Performance result
Heat affected zone (HAZ)	Heat affected zone is a layer, just below the recast layer, which has been subjected to the high temperatures of electrical discharge such that material did not melt but sufficient enough to cause a phase transformation, similar to that of heat treatment processes. The discharge energy magnitude influences HAZ [68, 69].
Micro-crack density	Micro-crack density defined as the severity of micro-crack exists on the machined surface. These micro-cracks typically found in the recast layer but rarely extended beyond the recast layer. It has been found that discharge current and pulse combination pairs are having more dominant effect on micro-crack density compared to discharge energy [69]

The selection of process parameters combination for obtaining consistent machining performance in EDM is a challenging task due to the stochastic nature of EDM process and complex relationship between process parameters and process performance. Therefore, studies have been conducted to identify optimal process parameter combination by process analysis [70, 71]. Moreover, process modelling studies have been done to form expression between process performance and process parameters in order to better control the EDM process and predict its performance results [72, 73].

2.1.3 Comparison of Conventional (macro) EDM and micro-EDM

Micro-EDM is derived from macro EDM by reducing the discharge energy and enhancing the positioning accuracy. The working principle of Micro-EDM is similar to conventional (macro) EDM. The differences between these two are summarized in table

2.3

Table 2.3 Comparison between micro-EDM and conventional EDM [9]

Conventional (macro) EDM	Micro-EDM
Typically used to machine large hole or pocket ($>500 \mu\text{m}$)	Typically used to machine small hole or pocket ($< 500 \mu\text{m}$)
The discharge gap distance between tool electrode and workpiece is large ($>10 \mu\text{m}$)	The discharge gap distance between tool electrode and workpiece is small ($< 10 \mu\text{m}$)
Pulse on time in conventional macro EDM is large ($> 1 \mu\text{s}$)	Pulse on time in Micro-EDM is small ($< 1 \mu\text{s}$)
Peak current is large ($> 3.5 \text{ A}$)	Peak current is small ($< 3.5 \text{ A}$)
Discharge energy is large ($> 25\mu\text{J}$)	Discharge energy is small ($< 25\mu\text{J}$)
The material removal rate in macro EDM is high	The material removal rate in micro-EDM is low
Jet flushing method is typically employed in EDM	Electrode rotation technique is employed for flushing
Conventional (macro) EDM	Micro-EDM
The need of tool electrode precision and the clamping system (repeat accuracy) in conventional EDM is not high	The need of tool electrode precision and the clamping system (repeat accuracy) in Micro-EDM is very high ($\square 1\mu\text{m}$)

Erosion rate in conventional EDM can be maximized within the allowable surface tolerances	Surface roughness in Micro-EDM can be optimized within the erosion rate tolerances
---	--

2.2 Process modelling in EDM and micro-EDM

Researchers have conducted both theoretical and empirical studies to investigate the influence of process parameters on the process performance in EDM and Micro-EDM. These studies help in formulating the process models, which are useful in improving the process performance through the selection of parameters according to the desired machining outcome [19], and in obtaining the required quantitative relation for on-line adaptive control of the EDM process [18]. The models which are formulated by theoretical approach uses equations based on universal principles. These basic equations are then combined with equations of state that are estimated using empirical data. On the other hand, the models formulated by empirical approach uses empirical data obtained from different statistical methods, such as Taguchi method [15], response surface methodology [74], regression modelling [73], factorial design method [69], forecasting method such as artificial neural network [75] and residual grey dynamic model [72]. Although both theoretical and empirical models have been developed in order to predict the performance measures and process control, only theoretical models have the capability to address underlying principles and the physics behind the material removal mechanism in the process. Therefore, a theoretical approach was used in this work for modelling of the crater size of anode and review on theoretical modelling was done.

In order to determine crater size and performance measures in a single discharge EDM and Micro-EDM process, it is important to perform the heat conduction analysis due to heat input from a single discharge. Although both numerical and analytical modelling approaches can be used in order to obtain solutions for heat conduction analysis, numerical approach provide greater flexibility in applying thermal loadings, boundary conditions and material properties. However, in the analysis of heat conduction using both these approaches requires fundamental parameters such as characteristics of heat source and heat flux, duration of time for heat application and material properties. Based on process characteristics, modelling can be divided into three regions, namely, cathode erosion, anode erosion and plasma channel.

An electro-thermal model was developed for EDM, in which a disk shape heat source was used to simulate the thermal heat input into the workpiece, which was assumed as a semi infinite cylinder [76]. The fraction of discharge energy transferred to workpiece and tool was assumed to be equal i.e. 50% ($F_c = 0.5$). The radius of heat flux and the thermophysical properties of the workpiece material over the whole temperature range were assumed as constant. The result of the temperature distribution of this model was found as a bowl shape with a nearly flat bottom surface. It was found that the calculated melting point isothermals were in good agreement with measured cross section of craters.

A two dimensional heat flow erosion model was proposed for workpiece material. In this model infinite and finite cylindrical surface for workpiece in the radial direction was assumed [77]. The heat source was assumed as circular shape and also fraction of discharge energy transferred to both electrodes was assumed equal i.e. 50%. However, the analysis was done only in finite z direction, as this model was very similar to Snoey's

model (Snoey and Van Dijck, 1971). The characteristics of temperature distribution of this model were found to be similar to Snoey's model with larger affected surface distance for same temperature [78].

A model using a semi-infinite cylinder surface for workpiece with a disk shaped heat source was developed [79, 80]. However, this model was not specifically developed for the EDM process and constant heat flux, as the heat input was assumed without taking the account of fraction energy transferred to the workpiece. This model's temperature distribution results were found to be almost similar with Snoey's model [78].

An erosion model was presented by assuming a uniformly disc shaped heat source situated between two semi-infinite bodies (tool and electrode) and time dependant heat flux radius for single spark EDM [16, 58, 81]. This model assumed that conduction is the only medium for heat transfer from plasma channel to tool and workpiece. The fraction of total energy liberated through the conduction across the discharge gap was assumed as 90% and equally distributed to workpiece and tool ($F_c = 0.5$). This model yields accurate results for depth-to-diameter ratio of craters with experimental results due to incorporation of growing plasma channel.

A hybrid thermal model was developed by integrating empirical equation obtained using a stochastic methodology called Data Dependent Systems (DDS) [82], with heat conduction equation solved for transient temperature distribution. This temperature distribution was used to determine material melting temperature isotherm, which represents the geometry of characteristic crater. Based on the geometry of crater, the erosion rate per discharge was predicted.

A one dimensional heat flow cathode erosion model was developed by using point heat source which accepts power rather than temperature as the boundary condition at plasma channel/cathode interface instead of a disk shape for conduction [59]. The fraction of total power transferred to cathode was assumed as 18% ($F_c = 0.18$). This fraction power was measured using a current signal measurement from highly precision data. The average thermophysical properties of the material were applied over the temperature range from solid to liquid state. The resulting temperature profile obtained was spherical.

An electro-thermal model for anode erosion was proposed by utilizing an expanding circular heat source which accepts power rather than temperature as boundary condition at plasma channel/cathode interface for conduction [83]. The fraction of total power transferred to anode was assumed as 8% ($F_a = 0.8 \%$). This model considered Gaussian distributed heat flux on the surface of anode, which is assumed to be produced by supplied power and grow with time. The model estimated not only the rapid melting of anode material but also subsequent resolidification of the material for longer pulse on time.

A variable mass, cylindrical plasma model was developed which expands with time for EDM spark process in liquid media [53]. This model estimated plasma enthalpy, mass density by incorporating thermophysical property subroutine and particle fraction by inclusion of the heats of dissociation and ionization for plasma created from demonized water as dielectric medium. This model provides important plasma parameters such plasma radius, temperature, plasma pressure, plasma mass and power fraction transferred

to plasma. This model estimated unique high pressure which showed that superheating is the dominant factor for EDM spark erosion.

A model based on Finite Element Method was presented to predict material removal rate and depth of damaged layer [84]. This method was used to solve heat conduction equation for workpiece due to melting and simulations for single spark in the form of pulses. It was assumed that width and depth of formed crater depends on spark-radius and power intensity. The model estimated that MRR increases with power per cycle and decreases with an increase in machining cycle time.

A model based on electro-mechanical mechanism was proposed for EDM process [54]. This model estimated that the electrostatic force was an important factor in material removal for short pulse on time duration below $5\mu\text{s}$ and considers thermal melting effects as insignificant in short pulse duration.

A model based on Finite Element Method was developed by using discharge power as boundary condition using commercial software called DEFROM to predict temperature distribution, material transformation, residual stress and final crater shape for single spark EDM process using Eubank's data [85]. It was found that the final shape of crater from DEFROM simulation result had depression in the middle with edges. However, the theoretical crater size by this model study had not compared with experimental crater size.

A thermal-electrical model was presented based on Joule heating effect in the discharge channel using Finite Element Analysis for a single discharge EDM process [86]. This model assumed equivalent heat input radius, which is dependent on current intensity and

pulse duration. The thermo-physical properties of material used in this model assumed as average of both ambient and melting value. The resulting melting volume per discharge pulse was compared with experimental result of the Agie SIT data [59]. The author reported that Joule heating effect is the main source of thermal energy to increase discharge channel temperature and melting of both the electrodes.

A non-linear, transient, thermo-physical model was developed to predict the shape of crater cavity and material removal rate for single spark die sinking EDM process using Finite Element Method (FEM) [87]. This model considered realistic assumptions such as Gaussian distribution of heat flux, spark radius based on discharge current and discharge duration, and latent heat of melting. It has been reported that energy distribution factor for cathode varies with energy zones such as 0.183 for lower energy zones (up to 100 mJ) and 0.183-0.2 for medium energy zone (100-650 mJ). It was found that MRR values and crater cavity shapes predicted by this model were closer to the experimental results.

Although the theoretical models for both EDM and Micro-EDM share similar underlying principles, there are differences in electrical discharge characteristics for these two processes in terms of discharge energy, pulse on time and time variation of discharge voltage and current. Therefore, these factors causes' variations in modelling Micro-EDM in terms of thermal loading characteristics, boundary conditions and equation of states; which consequently influence final process performance results.

An analytical plasma channel model was presented for a single discharge Micro-EDM process [57]. This model incorporated various pre-breakdown phenomena such as current emission and bubble nucleation at micro-peaks in order to predict plasma temperature

and plasma pressure. The estimated plasma temperature and plasma pressure were found in the range of 8100 ± 1750 K and 6-8 bars respectively. However, this model did not cover anode and cathode erosion for Micro-EDM in order to estimate the performance measures such as MRR, TWR and surface roughness.

A mathematical model was developed based on heat transfer principles, which was solved using commercial available finite element method to estimate the crater size, temperature distribution on the workpiece and residual stress on and near the crater for a single spark Micro-EDM process [88]. This model assumed the constant heat input radius with a Gaussian heat distributed heat source. The thermo-physical properties of material used in this model assumed as temperature dependent. The fraction of total energy transferred to anode was assumed as constant i.e. 8 % ($F=0.08$). The simulated crater dimensions and residual stresses were compared with experimental values. It was found that simulated residual stresses near the crater exceeds the ultimate strength near the spark center and decreases with increases in distance from center. However, simulated crater size was found to be much smaller than experimental crater size.

A MATLAB and FEA based thermo-numerical model was presented, which simulated the material removal mechanism and residual stress for a single discharge Micro-EDM machining on Molybdenum [89]. However, the spark radius for this model was assumed to be constant. The fraction of total energy transferred to anode was assumed constant i.e. 8 % ($F=0.08$). This model studied the effect of important EDM parameters such as pulse duration on crater dimension and tool wear percentage. This model compared simulated crater size with experimental data which showed that size of crater can be effectively approximated using thermo-numerical method for a single discharge Micro-EDM

process. It was found that percentage of tool wear decreases with an increase in the pulse duration. A coupled thermal-structural finite element analysis showed that tensile residual stresses build up near the crater boundary in all directions causing surface damage such as micro-cracks. In this process the input energy range of 60 μJ to 600 μJ was used.

A theoretical model was proposed, which solved the thermal conduction equation by an analytical approximation approach using process parameter settings, within a range of 5 μJ to 150 μJ for predicting Micro-EDM process performance measures such as MRR, TWR and surface roughness, based on the geometry of a single crater [90]. The correction factors were determined by comparing performance measure values with corresponding measured values. These correction factors could be then used to recalibrate performance measure values in order to approximate analytical performance values with empirical values.

A theoretical model was proposed based on electro-thermal material removal mechanism for single discharge Micro-EDM [91]. In this model, an expanding circular heat source with time-varying heat flux was used as the thermal loading condition for heat conduction analysis. This heat conduction model was solved using finite element methods. This analysis showed that the plasma flushing efficiencies (PFEs) at the anode for discharge energies of 1.6 μJ , 3.4 μJ and 14.6 μJ were found to be in a range of 19%, 23% and 33% respectively.

2.3 Conclusion of Literature Review

The process models developed based on theoretical approach provides not only the relation between process parameter and process performance to predict performance parameter but it also helps to better understand material removal mechanism during machining. Based on the results of studies conducted, there are certain gaps in modelling of micro-EDM process.

1. Limited studies have been carried out in anode process modelling and simulation for micro-EDM when the discharge energy is less than 1 μJ and pulse on time less than 50 nanoseconds.
2. Heat input radius equal to crater radius has not been considered in previous electro-thermal modelling approach.

CHAPTER 3

EXPERIMENTAL METHODS AND MEASUREMENT TECHNIQUES FOR SINGLE SPARK ANALYSIS

3.1 EXPERIMENTAL OBJECTIVES

To better understand single spark analysis, it is necessary to identify and understand the factors affecting the crater size. The factors affecting the crater sizes have been studied by conducting series of machining experiments. This chapter initially covers the experimental set up for single spark analysis on micro-EDM. The experimental setup

consists of single discharge experiment, workpiece, tool electrode and dielectric. Later the methods used in preparation of workpiece samples and the measurement of performance parameters are discussed.

3.2 Experimental setup

The experimental setup includes equipment and materials used in performing micro-EDM experiments. Based on experimental objectives, equipment's and materials were selected.

3.2.1 Micro-EDM MACHINE

The commercial Panasonic micro-EDM machine (MG-ED72W) operated with CNC Control system was used to conduct single discharge experiments with different machining parameters such as discharge energy and discharge gap distance. This unit can generate single pulse discharge resulting in distinct and ordered craters at different locations. Also, this unit equipped with data acquisition system to capture electrical parameters of each discharge so that resulting craters could be studied in relation to machining and discharge parameter used. Figure 3.1 shows the micro-EDM set up used in this for experiment. The features of machine are listed below.

3.2.1 Tool Electrode – The tool electrode is placed inside mandrel and the tool is ground to a precision on the orders of micrometers. This mandrel linked to V shaped ceramic bearing through belt connection. This belt connection enables the rotation of tool electrode with minimum eccentricity and alignment through a variable speed motor attached to mandrel. A built in wire electrical discharge grinder facilitate to reduce the

diameter of tool electrode to a required diameter and most importantly responsible for reducing eccentricities on the tool electrode.

3.2.2 X-Y table – This X-Y table consists of dielectric tank. A closed loop NC control system drives this stage at $0.1 \mu\text{m}$ using stepper motor and a ball screw attachment with glass scale positioning sensor. The workpiece is placed inside the dielectric tank.

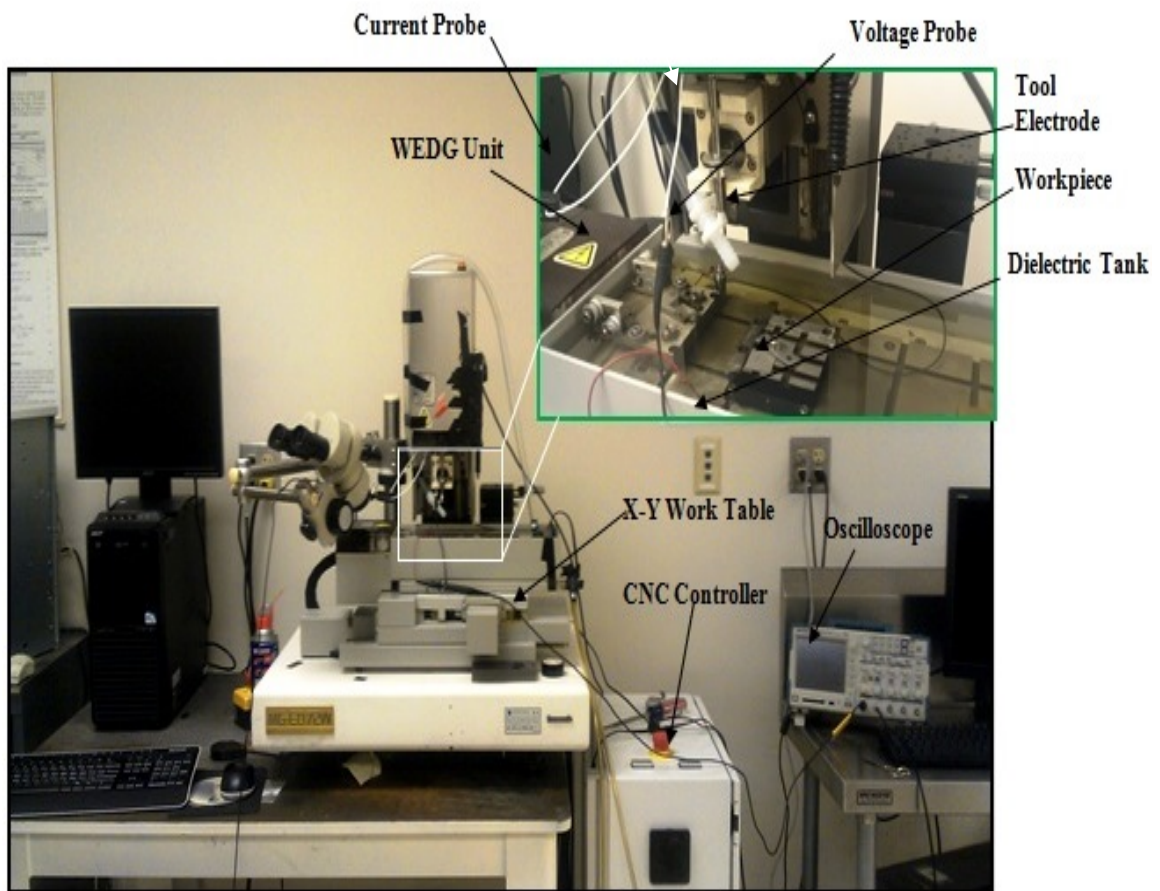
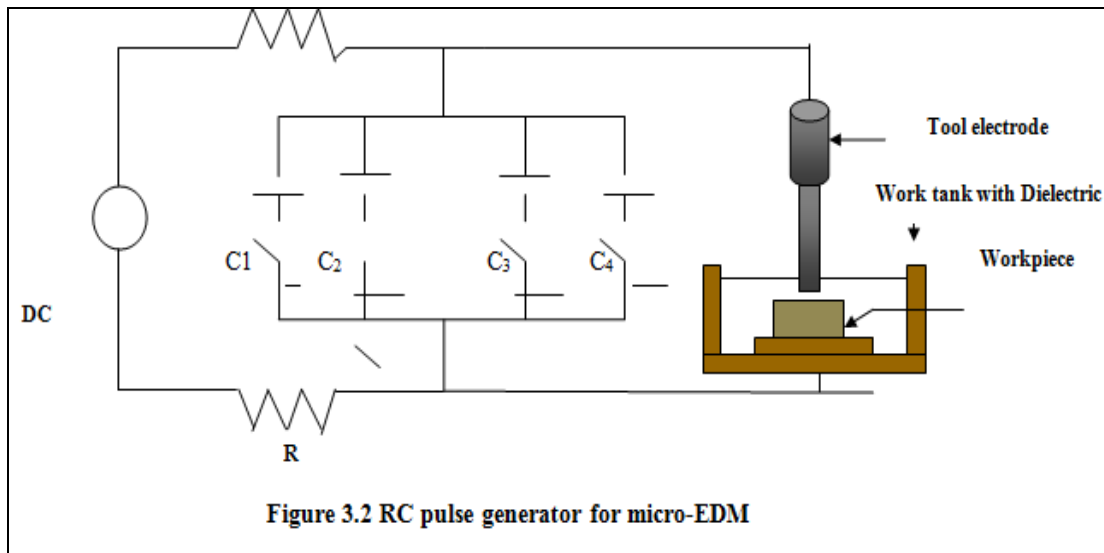


Figure 3.1 Micro-EDM machine

The pulse generator in micro-EDM machine (MG-ED72W) is relaxation-capacitance (RC) circuit as shown in figure 3.2 consisting of open circuit voltage which could be set from 0V to 120V, resistor labeled R and four capacitors setting labeled as C_1 , C_2 , C_3 and

C_4 with capacitance values of 3300pF, 200pF, 100pF and 0pF, respectively. The tool electrode could be rotated at 3000 rev/min. Conventional polarity arrangement in micro-EDM could be selected through a connecting RC pulse generator to tool electrode and anode such a way that tool electrode is place as cathode and workpiece as anode.



The following are key points about the relaxation circuit.

1. The construction of the power generator is simple and robust.
2. A very small energy is stably achieved with small pulse duration
3. The material removal rate is low because of the time required to charge the capacitor.
4. It is difficult to obtain uniform surface finish due to varying discharge energy.
5. There is possibility of thermal damage on the workpiece if dielectric strength is not recovered after previous discharge.

In spite of these limitations, the RC pulse generator can generate small discharge energy by selecting minimum capacitance value in the circuit, and hence is widely applied in micro-EDM.

3.2.3 Work piece and tool electrode

The work piece material used in the experiment was titanium alloy (Ti-6Al-4V, grade 5). The chemical compositions of the workpiece material are shown in Table while its thermo-physical properties are shown in Table. The dimension of workpiece sample is 20mm X 20mm X 1mm.

Table 3.1 Chemical composition of titanium material

Workpiece material	Typical chemical composition (%)				
Titanium	Al	Fe	O	Ti	V
	6	0.25	0.2	90	4

Table 3.2 Thermo-physical properties of titanium material

Property	Workpiece material
	Titanium
Density, ρ (kg/m ³)	4430
Thermal Conductivity, K (W/m.K)	6.7
Specific Heat, c (J/kg.K)	4430
Melting Temperature, T _m (K)	526.3

3.3 Work piece preparation

Before conducting experiment, the workpiece sample was pre-polished to achieve a mirror surface finish in order to detect distinct single discharge crater. A reference plane with different slots was made on workpiece. Then by machining at predefined locations the distinct crater size with different energy levels are were revealed and measured under SEM.

The tool electrode used in the experiment was tungsten wire electrode with diameter of 125 μm . In order to detect distinct single discharge crater the diameter of 125 μm was reduced to diameter of 100 μm using wire electro discharge grinding (WEDG) system. While performing experiments for single discharge, the tool electrode was rotated at a speed of 1000rev/min.

3.4 Characterization techniques

Characterization technique infer to the measurement and inspection methods which are used to measure and/or investigate the features of interest in terms of quantitative and qualitative manner. This section covers equipment used to calculate the experimental performance values related to the research.

3.4.1 Voltage and current probes with oscilloscope

In order to capture changes in voltage and current during electrical discharge duration, voltage and current probes were used. All the voltage and current changes recorded through waveforms are displayed quantitatively on the oscilloscope. The electrical discharge data acquisition system consists of TektronixP5205 voltage probe, Tektronix A6302 current probe and Tektronix TDS2022 oscilloscope with sampling frequency of 2

giga-samples per second. This high sampling frequency is necessary to minimize the issue related to aliasing, especially when duration of discharge is in sub-nanosecond range. The machining parameters such as breakdown voltage, average discharge voltage, average discharge current, peak discharge current and pulse on time are the important crucial factors in better understanding the discharge mechanism and for calculation of total discharge energy in micro-EDM. These factors can be obtained through discharge voltage and discharge current waveforms captured using the voltage and current probes. These waveforms can be displayed on the oscilloscope. A typical voltage and current waveform is illustrated in figure 3.3

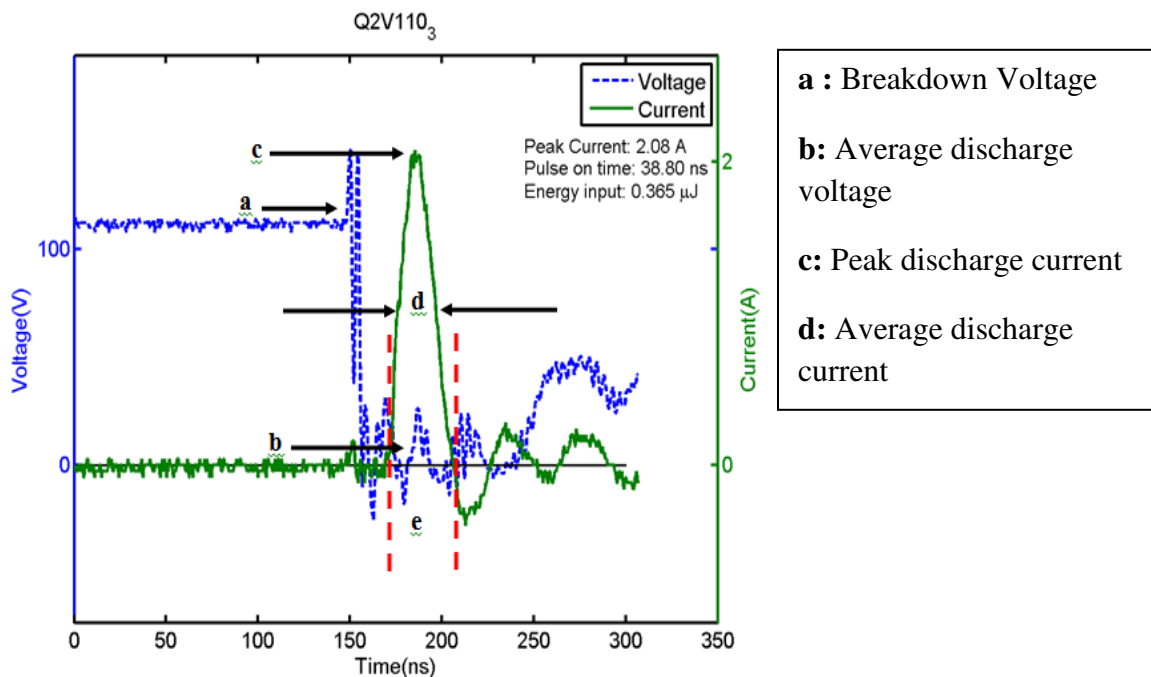


Figure 3.3 Typical voltage and current waveforms

The above mentioned breakdown voltage represents the voltage measured across discharge gap just before dielectric breakdown. This breakdown voltage can be equal to or smaller than the open circuit voltage (V_{oc}).

The following equations are used to compute the values of average discharge voltage and current, by time averaging total discharge voltage and current over the pulse on time.

$$V_{av} = \frac{1}{t_2 - t_1} \int_{t_1}^{t_2} v(t) dt \quad (3.1)$$

$$I_{av} = \frac{1}{t_2 - t_1} \int_{t_1}^{t_2} I(t) dt \quad (3.2)$$

Where V_{av} represents the average discharge voltage, I_{av} represents average discharge current, $V(t)$ represents voltage as function of time, $I(t)$ represent current as a function of time, t_1 and t_2 represents start and end of pulse on time respectively.

Also, the input discharge energy and measured energy can be computed using equations (3.3) and (3.4), respectively

$$E_{in} = \frac{1}{2} \cdot C \cdot V_{OC}^2 \quad (3.3)$$

$$E_m = \int_{t_1}^{t_2} V(t)I(t) dt \quad (3.4)$$

Where E_{in} represents as input discharge energy, E_m represents as measured discharge energy, C represents as selected capacitance and V_{oc} represents as open circuit voltage.

The measured discharge energy is computed from measured discharge voltage and current waveform. This can be expressed in the discretized form and its equation is as follow.

$$E_m = \sum_{i=1}^n V_i \cdot I_i \cdot \Delta t \quad (3.5)$$

where

$$\Delta t = \frac{t_2 - t_1}{n}$$

V_i represents the discretized discharge voltage at i^{th} time step, I_i the discretized discharge current at i^{th} time step and n the total number of time steps.

CHAPTER 4

PROCESS MODELLING AND SIMULATION

This chapter presents the results of numerical simulation conducted for micro-EDM process. The first section provides the purpose of developing single electrical discharge model for micro-EDM. Afterwards, the finite element method used for modelling and simulation is explained.

4.1 Single electrical discharge model for micro-EDM

Many researchers have attempted to describe the crater formation due to single electrical discharge in micro-EDM [57, 78, 90]. However, the discharge energy level in all the models was greater than 1 μ J. The purpose of model describing micro-EDM not only used to elucidate the mechanism of material removal, it may also serve as tools to predict process performance without the need of actually performing the experiments.

4.2 Modelling with finite element method

From earlier study it is evident that the material removal mechanism in EDM is stochastic in nature and it involves combination of several disciplines such as electrodynamics,

thermodynamics and hydrodynamics [92]. It is difficult to present simple and comprehensive model explaining the nature of process in detail. To overcome these complexities arising from multi-disciplined nature of process, there is need to make simplification to thermal loading and boundary conditions while developing material removal model which can be solved either by analytical or numerical methods. Analytical approach has a limitation of applying specific thermal loading and boundary condition. However, numerical approach provide greater flexibility in applying thermal loads, boundary conditions and material properties which helps to add wide range aspects of electrical discharge erosion process in order to investigate further insights into material removal process. In addition to these benefits, numerical approach shows various isothermal lines to identify different heat affected zones [93]. Finite element method is one of the numerical analysis methodologies implemented for investing process mechanism in EDM.

4.2.1 Physical description

The material removal in electro-thermal form of EDM can be modelled as superheating of workpiece electrode by incident of plasma channel formed between two electrodes, namely tool and workpiece. This results in to formation of crater on workpiece surface through thermal melting and vaporization. In the present work, cylindrical shaped plasma channel has been assumed. Due to axisymmetric nature of heat transfer between tool electrode and workpiece, a two dimensional model is assumed in the radial and axial coordinates of coordinates of the cylindrical system as shown in figure 4.1.

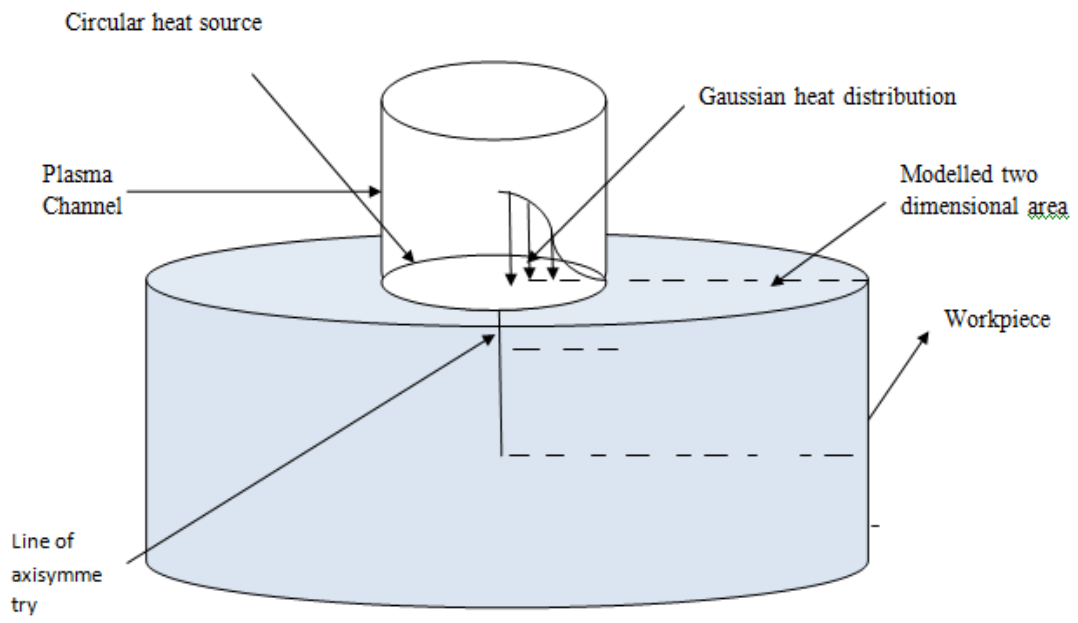


Figure 4.1 Schematic sketch of the physical model

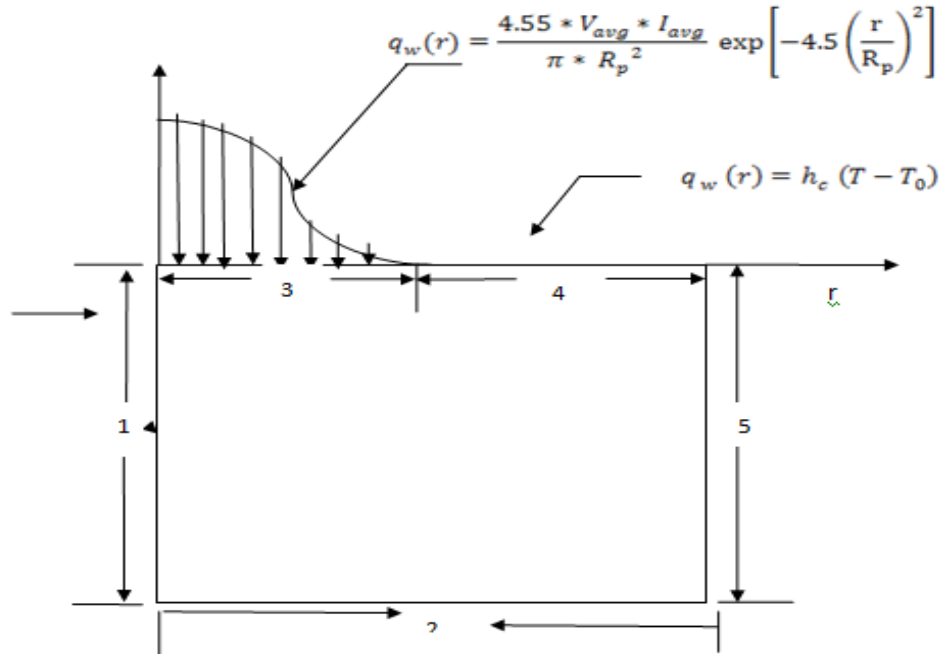


Figure 4.2 2D Model for micro-EDM process

EDM is a stochastic process because of the uncertainty arising due to factors such as plasma radius, shape of plasma channel heat source, energy distribution between workpiece and tool electrode. As a result it is difficult to incorporate the effect of all the parameters in the model for predicting crater size. The actual problem can be solved by making certain assumption.

Modelling involves following basic assumption were made

1. For the analysis only one spark is considered.
2. The domain is considered to be axisymmetric about r-z plane.
3. Heat transfer within workpiece surface is dissipated by conduction and by convection at workpiece-dielectric liquid interface.

4. Gaussian heat flux distribution is considered as heat source incident on the surface of workpiece material during the pulse on time.
5. The material properties of workpiece are considered as temperature independent.
6. Plasma radius is assumed to be equal to crater size.
7. The fraction of total discharge energy is distributed as heat input into workpiece; rest is lost into dielectric convection and radiation.
8. Tool and workpiece are considered to be isotropic and homogeneous in nature.
9. The ambient temperature is room temperature.
10. The transient type of analysis is considered for temperature.
11. The capacitor is fully charged and discharged during the process.

The important parameters which contribute to the accurate prediction by EDM models include amount of heat input, radius of plasma channel and the thermo-physical properties of the material. Mathematical equations of these elements are essential in thermal analysis of EDM using FEM method, which represents different aspects of electro-thermal material removal process. These equations include thermal conduction model, expression for plasma radius and heat flux.

4.2.2 Thermal conduction model

The governing equation used for heating of axisymmetric workpiece due to single spark without internal heat generation in terms of cylindrical coordinates is given by

$$\rho C_p \frac{\partial T}{\partial t} = \frac{1}{r} \frac{\partial}{\partial r} \left(k \frac{\partial T}{\partial r} \right) + \frac{\partial}{\partial z} \left(k \frac{\partial T}{\partial z} \right) \quad (4.1)$$

where ρ is the density, C_p is the specific heat capacity, T is the temperature, t is the time, k is the thermal conductivity of workpiece material and r and z are coordinate axes.

4.2.2.1 Heat source

In the modelling of single spark discharge, different characteristics of plasma channel have been used such as shape, size and time-dependent growth [94]. The theoretical prediction of amount of heat applied to workpiece depends upon idealized geometrical shapes of plasma channel. It is found that plasma channel radius in EDM is an expanding quantity and its radius changes with time and is given by [59]

$$R_p = kt^{3/4} \quad (4.2)$$

However, there is limitation for calculating this constant k in micro-EDM. Further, It was proposed that for precise simulation of electrical discharge erosion process circular shape and time dependent growth of plasma diameter should be considered [95]. Therefore, the circular shape plasma channel was assumed in finite element analysis (FEA) to simulate workpiece-material in this research work. However, measurement of plasma radius is extremely difficult due to high pulse frequency constraints [96]. It was suggested that plasma radius can be determined from crater radius [97]. Also, it was proposed that crater radius was equal to plasma radius [98]. Moreover, it was found that plasma radius becomes equal to crater radius with increase in pulse duration [13]. In present study, the

time dependent plasma radius was assumed to be constant and is equal to measured crater radius from single discharge experiment.

4.2.2.2 Heat flux

In the most of the published single spark mathematical modelling studies, researchers have considered uniform heat flux distribution within plasma channel transferred to workpiece. This application of uniform heat distribution on work piece is far from reality. This facts is evidence from the temperature distribution inside the plasma channel using spectroscopy technique [94, 99]. However, some researchers [87, 89, 100] have considered Gaussian distribution of heat flux. Assuming Gaussian heat flux distribution, the expression for heat flux $q_r(r)$ at radial distance from the axis of spark is given by [96]

$$q_r(r) = q_0 \exp\left\{-4.5\left(\frac{r}{R_p}\right)^2\right\} \quad (4.3)$$

Where q_0 is the maximum heat flux at ($r = 0$) which can be calculated as:

$$q_0 = \frac{4.55 F V I}{\pi R_p^2}$$

Where F represents the fraction of total energy distributed to the workpiece electrode, V the discharge voltage, I the discharge current and R_p the plasma radius. The heat flux parameters such as average discharge voltage and average discharge current can be determined empirically from discharge voltage, discharge current and pulse on time. The exponent -4.5 used in the above equation signifies that how flat the Gaussian heat flux is

[94]. With increase in the value of this exponent (0 for example) the heat flux distribution becomes very flat while for exponents lower than this value heat flux distribution is steep. The -4.5 value exponent used in the equation is in good agreement with measurement obtained using spectroscopy [94].

Fraction of total discharge energy F distributed to anode is important parameter as it determines the amount heat flux going to workpiece. It has been suggested that material properties of individual electrodes and pulse duration effect fraction total energy [96]. This fraction of energy can be determined empirically or theoretically. It was found that 34% of total energy transferred to workpiece by measuring electrode temperature during EDM process [18]. It has been estimated that 18% of total energy is distributed for EDM process [59]. It was suggested that the fraction of heat flux distributed to workpiece decreases with increase in pulse on time in micro-EDM process [101]. It was found that 10.37% of total energy is distributed to workpiece by measuring electrode temperature in micro-EDM process [102]. It was assumed 39% constant fraction of total heat flux transferred to workpiece for micro-EDM process [90]. In present work, F is taken as 0.39.

4.2.2.3 Boundary Condition

The schematic diagram of the simplified micro-EDM thermal model with applied conditions during pulse on time is shown in figure 4.2. During the pulse on time on top surface at $Z=0$, heat input transferred to workpiece is represented by the Gaussian heat flux distribution. This Gaussian heat flux distribution is applied up to the plasma radius R_p as shown in equation. Boundary 3 is modeled as convective boundary condition due to

the heat loss to the coolant. For other surfaces T_2 and T_3 , no heat transfer occurs as they are assumed to be too far away from heat source. Due to axis symmetry of boundary T_4 , heat transfer has been taken as zero as there is no gain or loss across this boundary. In the micro-EDM process, the workpiece is immersed in dielectric medium. Therefore an ambient temperature is applied on as initial condition to the whole domain.

Initial and boundary conditions are as follows

IC: at $t=0$

$$T(r, z, 0) = T_0$$

BC at $t \geq t_{on}$,

$$k \frac{\partial t}{\partial z} = q_w(r) = \frac{4.55 * F * V * I}{\pi * R_p^2} \exp \left[-4.5 * \left(\frac{r}{R_p} \right) \right]^2 \quad \text{when } R < r \text{ for boundary 3}$$

$$k \frac{\partial t}{\partial z} = q_w(r) = h_c (T - T_0) \quad \text{when } R > r \text{ for boundary 4}$$

$$\frac{\partial t}{\partial n} = 0 \quad \text{for boundary 1, 2 and 5}$$

Where n is the normal direction on the surface, h_f is coefficient of convective heat transfer at work-dielectric fluid interface and T_0 is the ambient temperature.

4.3 Numerical model

COMSOL is used to simulate a two dimensional thermal, finite element model based on heat transfer physics for of single spark micro-EDM. COMSOL is a Finite Element Analysis (FEA) software package that allows user to develop 2D models with associated boundary condition. This software allows the user to define material properties and

equation within program to yield accurate representation of the problem. Comsol post-processing function gives the user visual representation of data which helps in assessing the results.

The heat transfer module of Comsol is used to solve heat conduction equation for the transient response. Further, two dimensional axisymmetric geometry is created with assumption that heat source and resulting craters are axisymmetric about the center of circular heat source. Heat flux boundary condition was applied on boundary 3. The second was convection boundary condition applied on boundary 4. As boundary 2 and 5 are away from the heat source, room temperature boundary conditions were assigned. The boundary 1 which represents line of axisymmetry was considered as adiabatic boundary condition.

The domain is considered as to be a semi infinite object in which model dimensions are ten times the dimensions (radius and thickness) of plasma radius R_p , as there is no change is found in FEM result while considering larger semi-infinite boundary conditions of the domain.

Mapped meshing is carried out with more number of elements distributed at heat affected zone where high gradient temperature exists as shown in figure. The FEA mesh had total 4160 elements and 16909 nodes. The size of smallest element is of order $0.2 * 0.2 \mu\text{m}$.

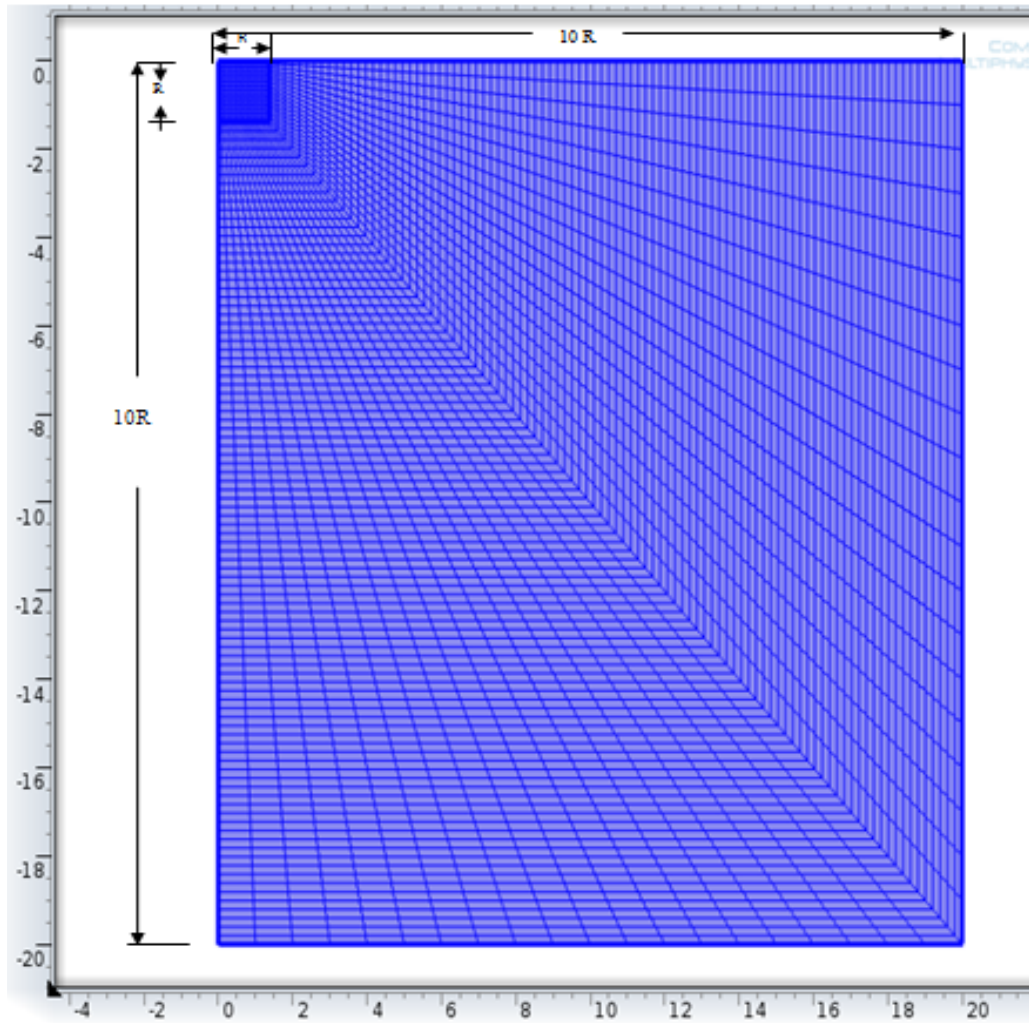


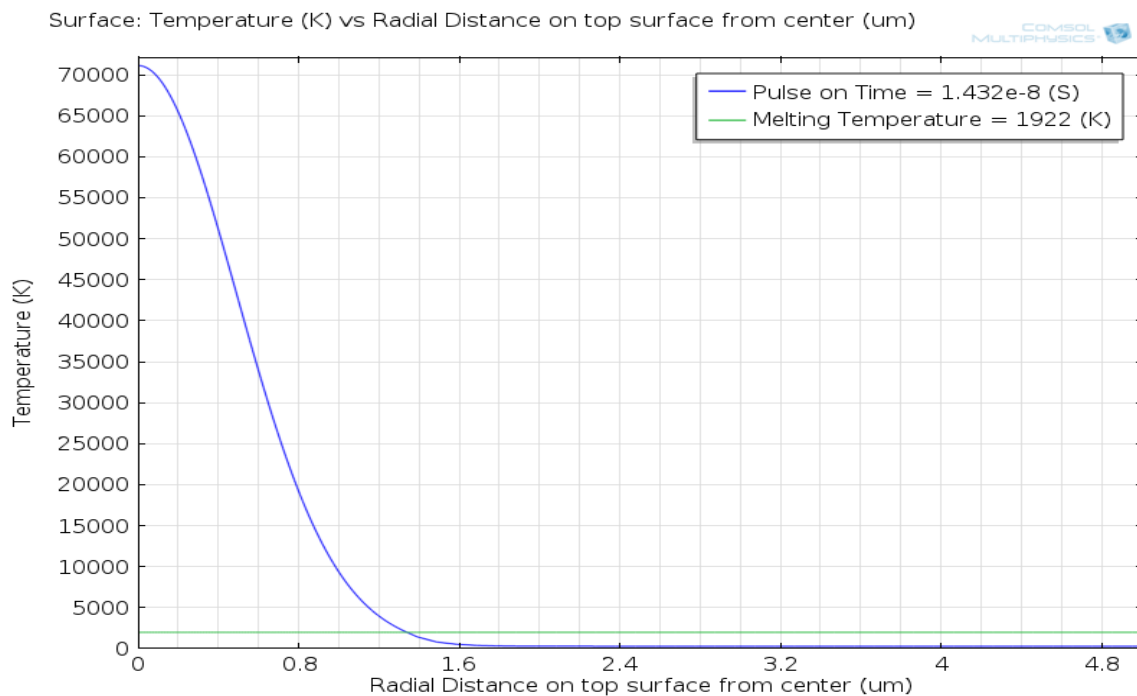
Figure 4.3 Mesh generation for FEM full model

4.4 Simulation Results and discussion

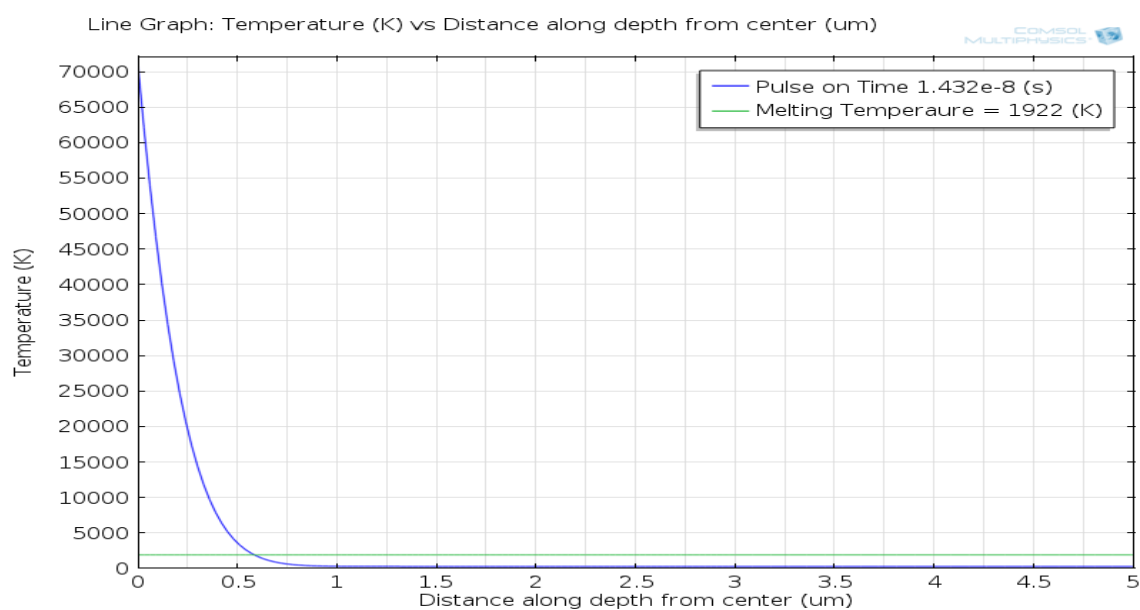
In this section FEM simulation results obtained during thermal model development were presented and discussed. Samples of simulated results were illustrated.

4.4.1 Temperature distribution

Figure 4.4a and 4.4b figure show temperature variation over the pulse on time obtained on top surface at a radial distance of 5 μm from center and at a of depth 2 μm from the top surface, i.e. along radial and axial directions for discharge condition I (0.1 μJ). From the figures, the radial distance on top surface and axial distance along depth showing temperature more than melting point were selected as removed part from material. Also it can be seen that change in temperature along the radial axis and vertical axis for any point has similar trends. Due to Gaussian heat source, the temperature is highest at origin and gradually decreases with increase in distance from center. Similarly the temperature distributions resulting from simulation of single discharge at discharge condition II to VI are shown in figure 4.5 to 4.9 figure.

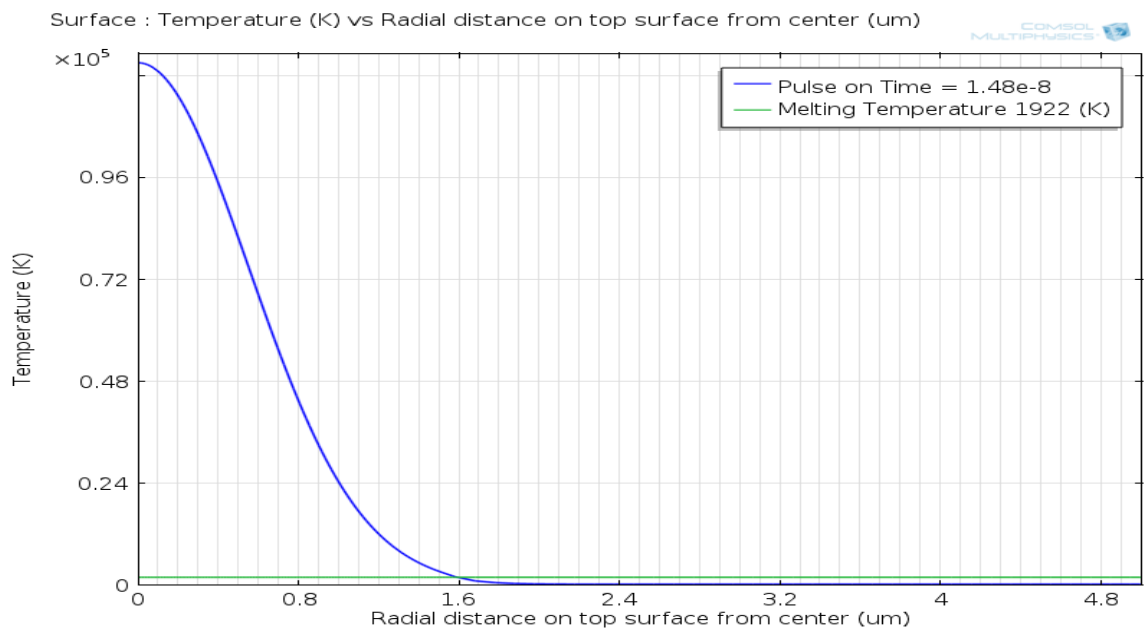


(a) Along radial axis

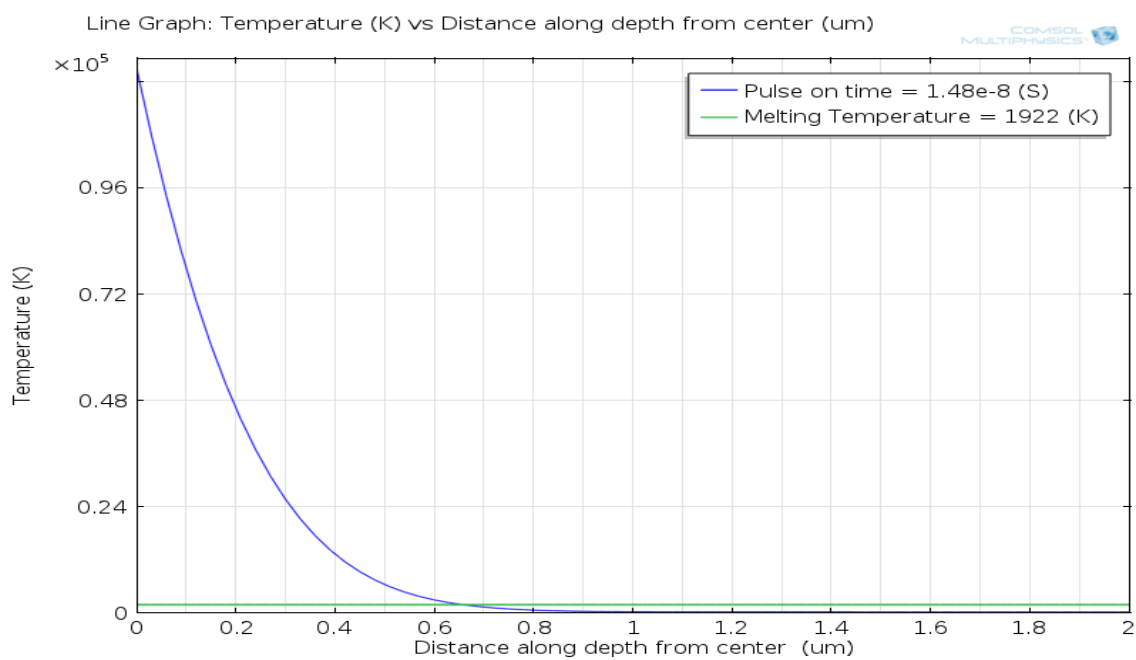


(b) Along vertical axis

Figure 4.4 Temperature variation with respect to distance for discharge condition I (0.1 μJ)

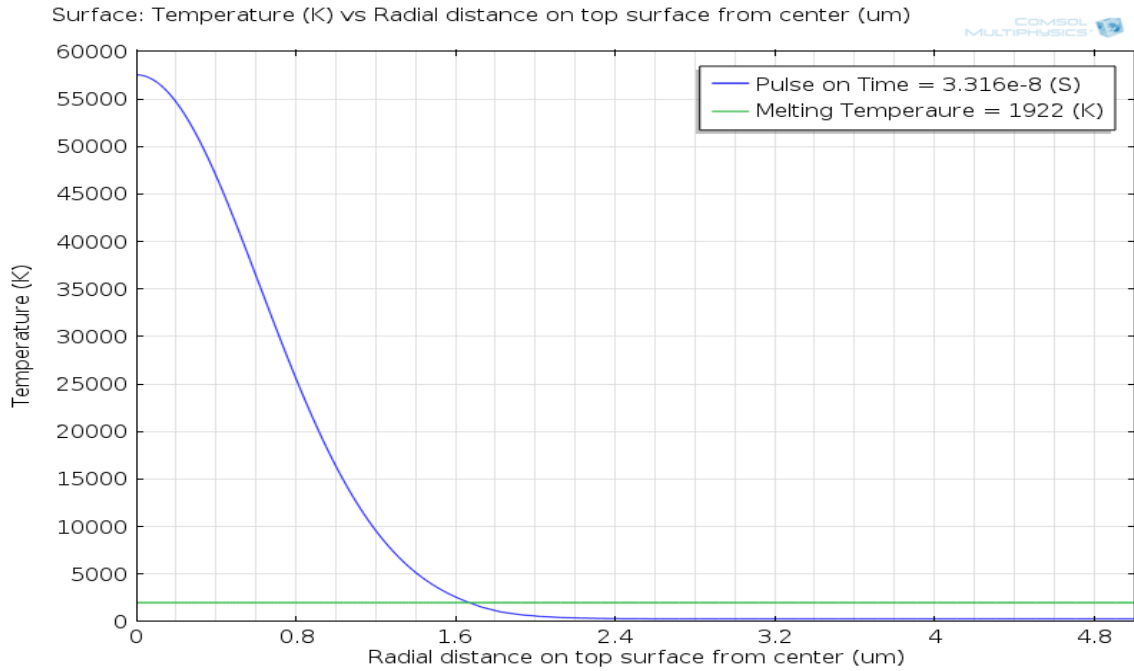


(a) Along radial axis

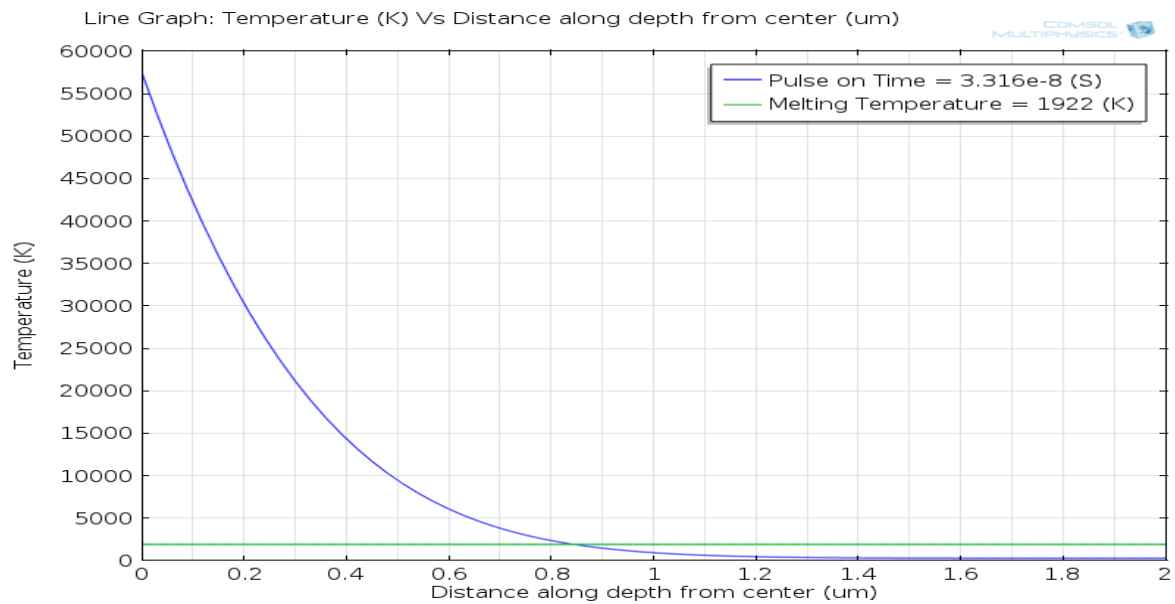


(b) Along vertical axis

Figure 4.5 Temperature variation with respect to distance for discharge condition II (0.238 μ J)

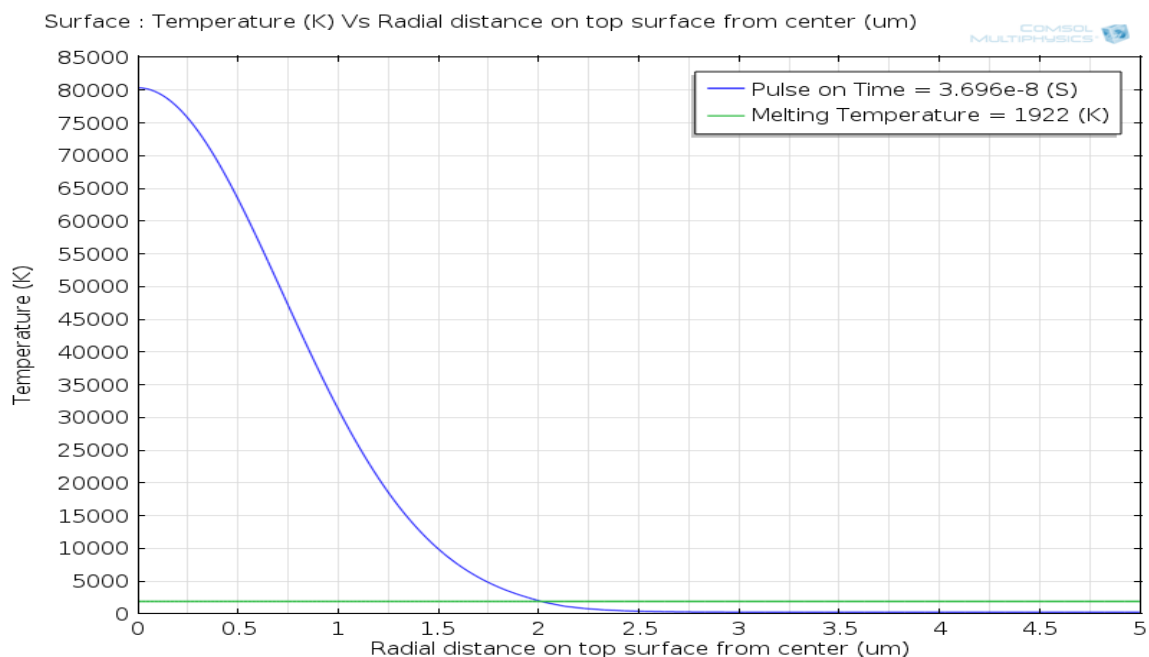


(a) Along radial axis

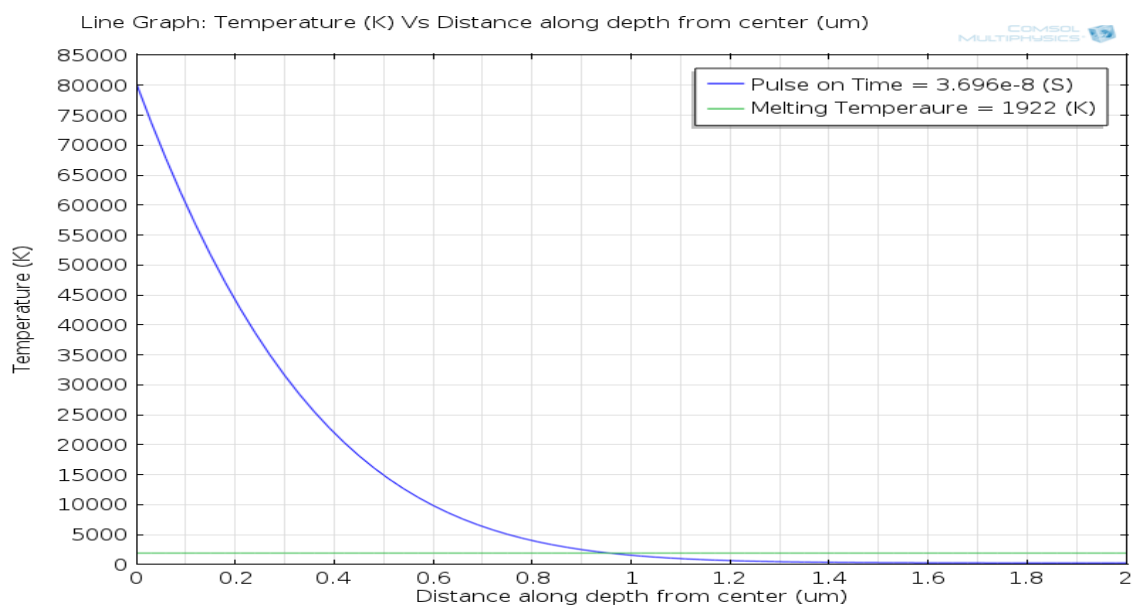


(b) Along vertical axis

Figure 4.6 Temperature variation with respect to distance for discharge condition III ($0.273 \mu\text{J}$)

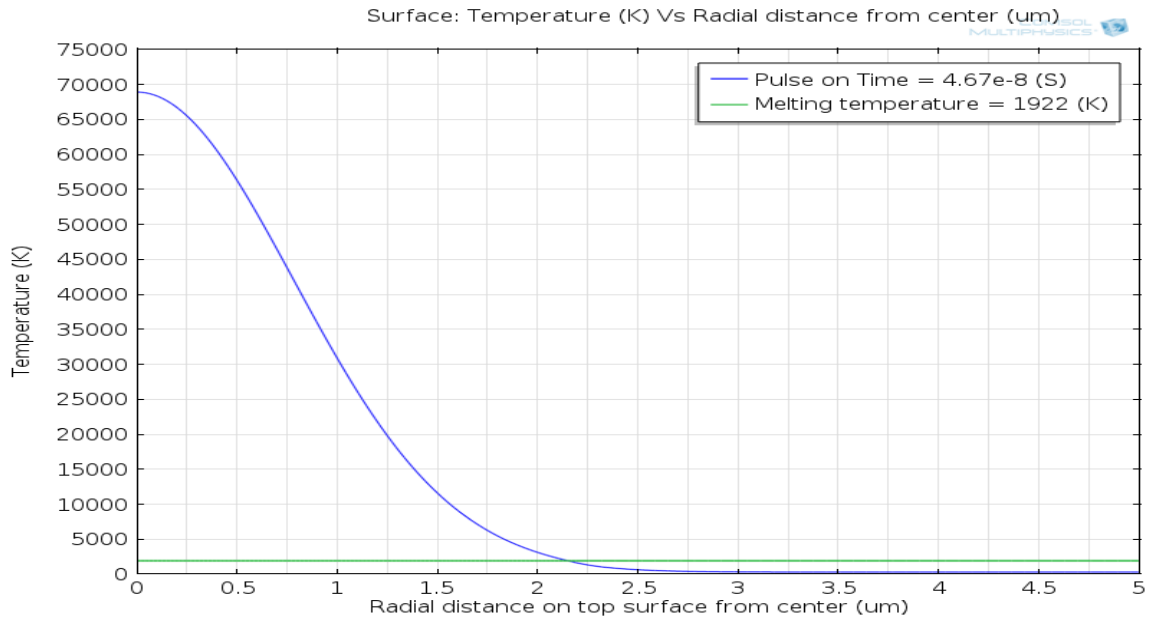


(a) Along radial axis

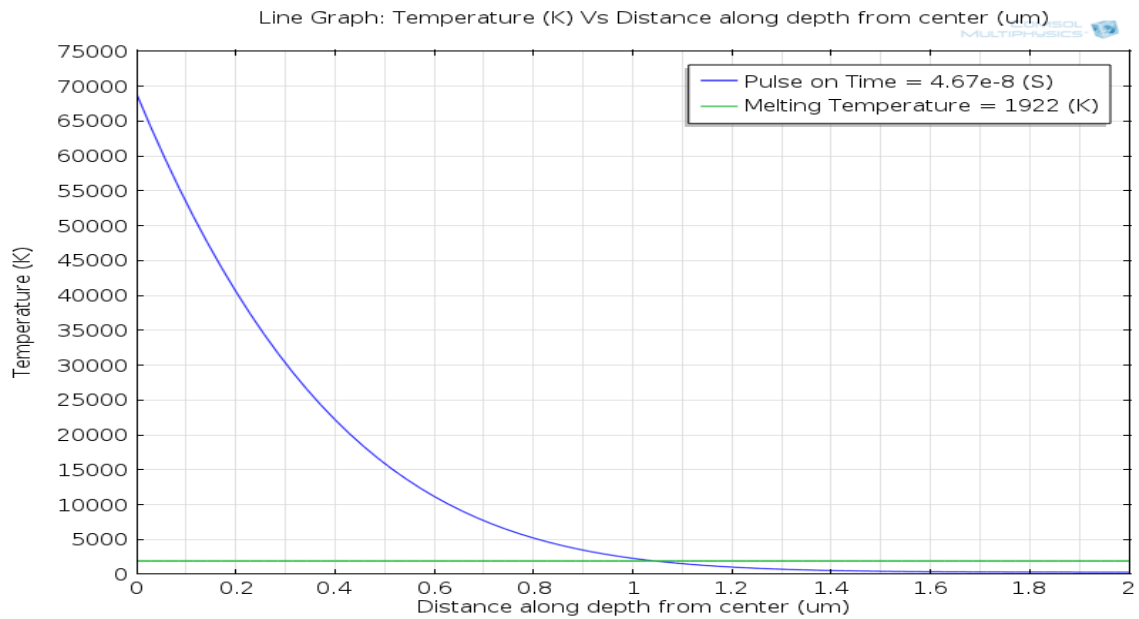


(b) Along vertical axis

Figure 4.7 Temperature variation with respect to distance for discharge condition IV ($0.373 \mu\text{J}$)

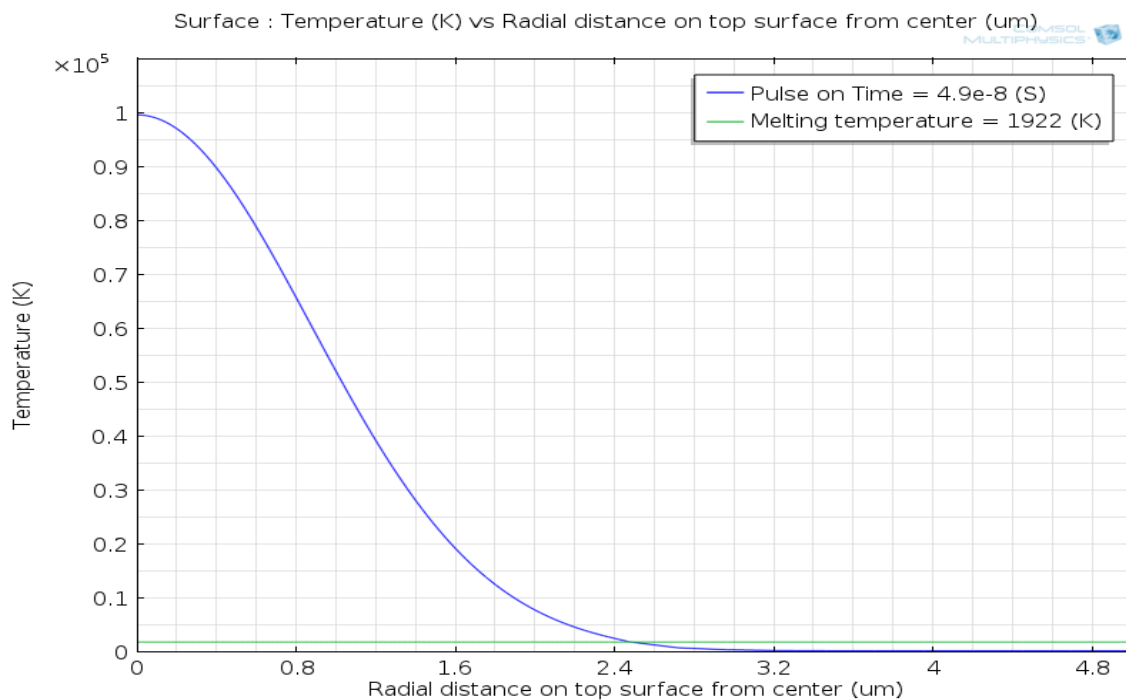


(a) Along radial axis

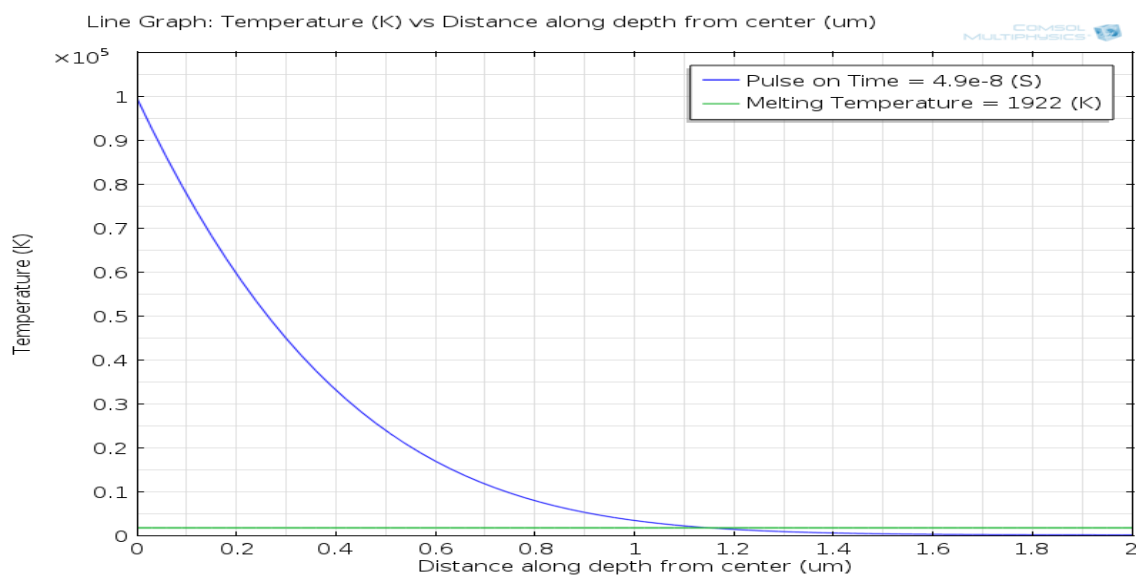


(b) Along vertical axis

Figure 4.8 Temperature variation with respect to distance for discharge condition V (0.6 μ J)



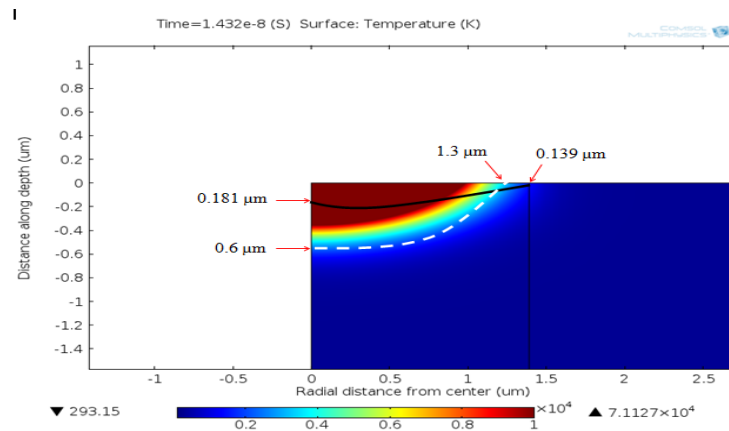
(a) Along radial axis



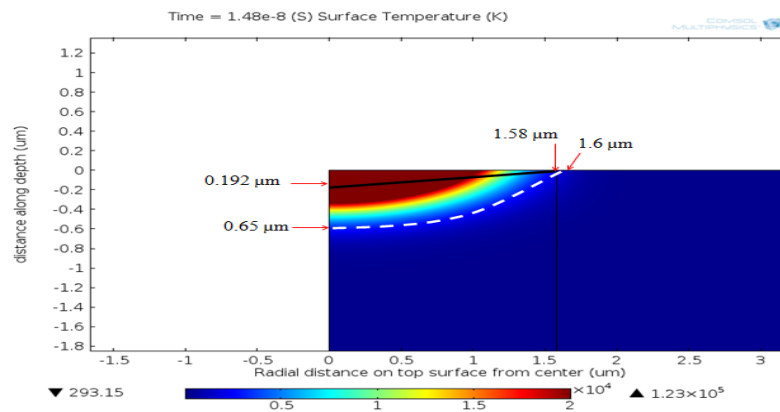
(b) Along vertical axis

Figure 4.9 Temperature variation with respect to distance for discharge condition VI (1.087 μ J)

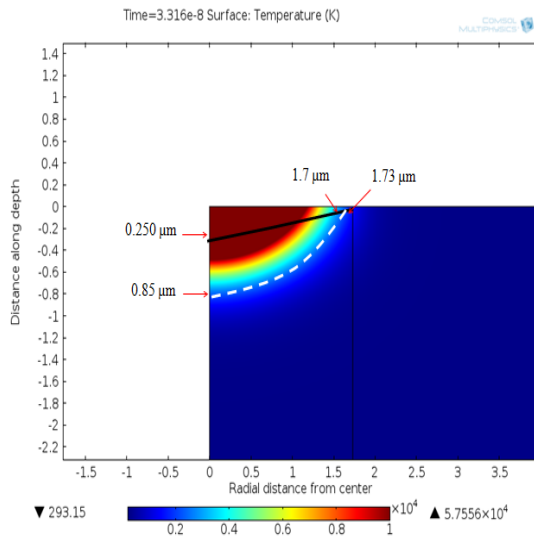
The FEM simulated thermal distributions of single electrical discharge at discharge condition I to II and III to VI are shown in figure 4.10 (a) to 4.10(b) and in figure 4.11 (c) to 4.11 (f) respectively. The dotted lines represents simulated melting isotherm and solid lines represents estimated crater profiles obtained from single discharge experiments. The estimated crater profiles obtained from experiments represented by circular arcs passing through measured radius and depth values.



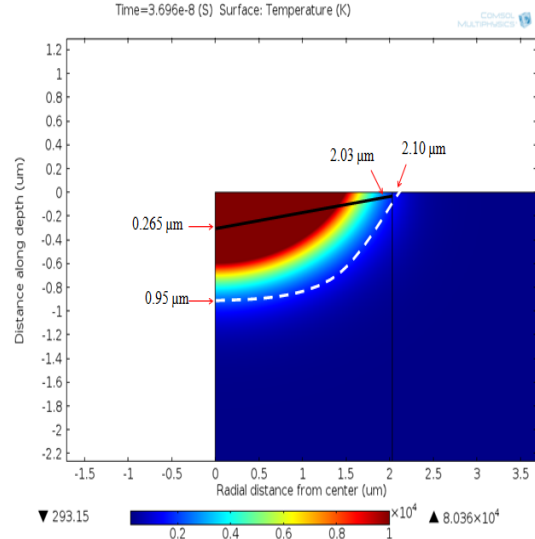
(a) Discharge condition I (0.1 μJ)



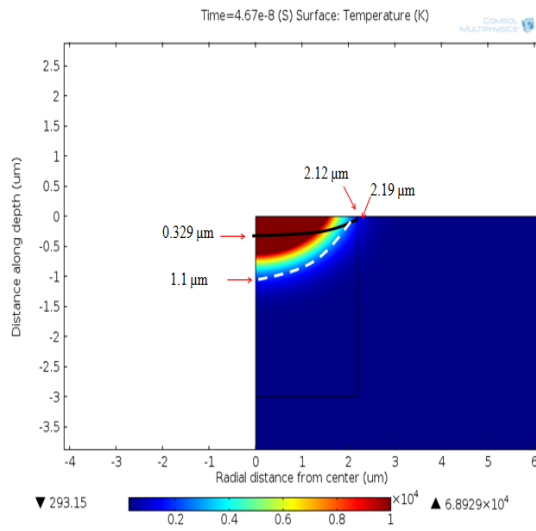
(b) Discharge condition II (0.238 μJ)



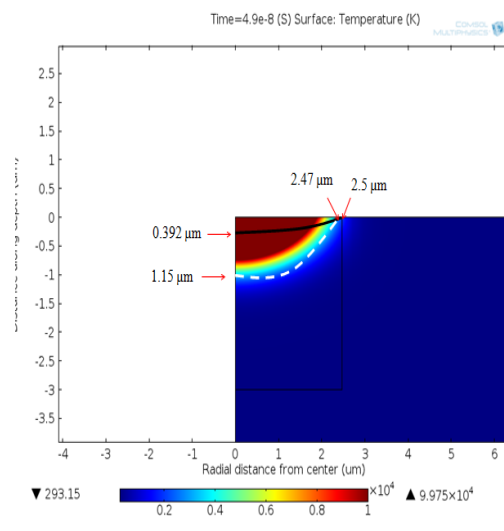
(c) Discharge condition III (0.273 μJ)



(d) Discharge condition IV (0.373 μJ)



(e) Discharge condition V (μJ)



(f) Discharge condition VI (μJ)

Figure 4.10 Thermal distribution for heat flux on a workpiece

CHAPTER 5

EXPERIMENTS

This chapter covers results of single spark experiment conducted to investigate the material removal mechanism in micro-EDM. The sparks are generated to form craters with different input energies typically engaging in micro-EDM. These formed craters used mainly to compare the results obtained by FEM simulation results. In this chapter advantages of single spark experiments are explained, followed by description of experimental method. Then, the effect of different process parameter on crater geometry, morphology and discharge waveform is discussed. Final section presents model verification by comparing simulation results with experimental results.

5.1 Single Spark experiment

To understand the effect of process parameters on material removal mechanism in micro-EDM, it is meaningful to investigate crater form due to the single spark of the process, under representative machining condition. Also this crater produced by one single spark pulse helps in improving machining precision. The single spark experiment is conducted to form non-overlapping craters and also to analyze individual craters produced by respective electrical discharge condition. This might help in building relationship between each recorded current and voltage waveform with resulting crater geometry and morphology. The crater diameter can be easily identified by forming single crater on smooth surface. This not only helps in measuring crater diameter accurately but also in observing crater morphology since single crater is more clearly visible as compared to multiple overlapping craters. Thus, the single spark experiment was conducted.

5.2 Experiment Design

The single discharge experiment was performed using three capacitance and open voltage levels of C1, C2, C3 and V1, V2 and V3 with the aim of studying effect of measured discharge energies on resulting crater size and morphology. Complete set of experiment parameters used in single spark experiment as shown in Table 5.1. The specific parameters for this study are measured discharge energy. Using combination of input parameters shown in Table 5.2, experimental runs were conducted and the outputs of crater were geometry were measured and discharge waveforms were recorded.

Table 5.1 Experimental parameters for single spark experiment

Parameter	Value
Open Voltage, V_{oc} (V)	70,110
Capacitance, C(pF)	10,100,220
Workpiece material	Titanium,
Tool electrode material	Tungsten
Tool electrode diameter (μm)	100

Table 5.2 Input parameters for each experimental run

Run	Discharge Condition	Capacitance (pF)	Open Voltage (V)	Input Energy (μJ)
1	I	10	70	0.0245
2	II	10	110	0.0605
3	III	100	70	0.245
4	IV	100	110	0.605
5	V	220	70	0.539
6	VI	220	110	1.331

Prior to start of the experiment, workpiece specimen was prepared by polishing so that small discharge craters can be distinguish from the original surface. The surface of workpiece was machined with marks in order to identify the single spark of a particular discharge condition. For each run appropriate capacitance and open circuit voltage was selected based on required input energy, defined as measured energy. To create a single spark crater, G28.1 surface detection function of micro-EDM machine was used. This generate some sparks while touching the workpiece surface which results in formation of cluster of sparsely distributed craters on workpiece surface with reasonable consistent size and shape. Figure 5.1 shows the example of crater cluster generated using discharge condition I for micro-EDM. Out of these craters produced on workpiece surface, single

crater can be used for the analysis. During this period the occurrence of successful electric spark can be verified by recorded current and voltage waveform on the oscilloscope.

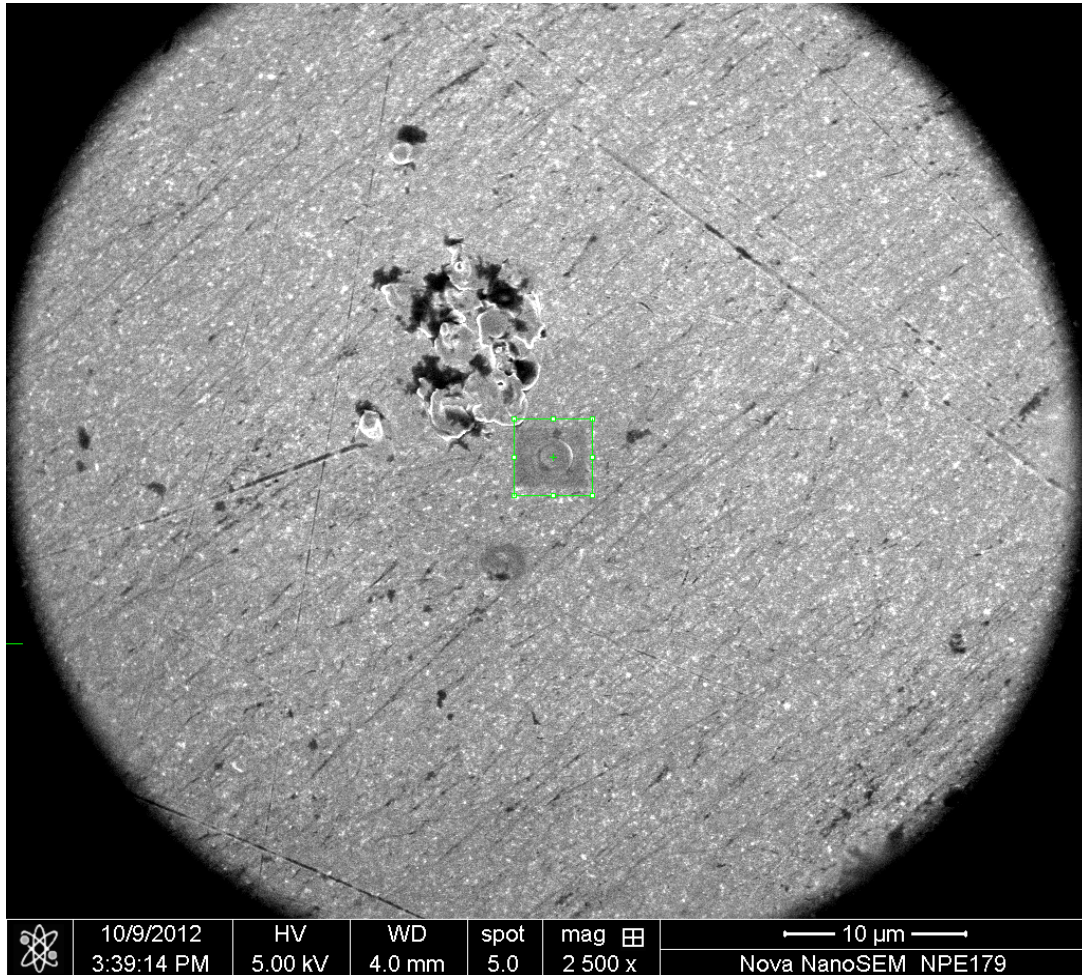


Figure 5.1 Discharge craters generated during discharge condition I

5.3 Experiment Results and Discussion

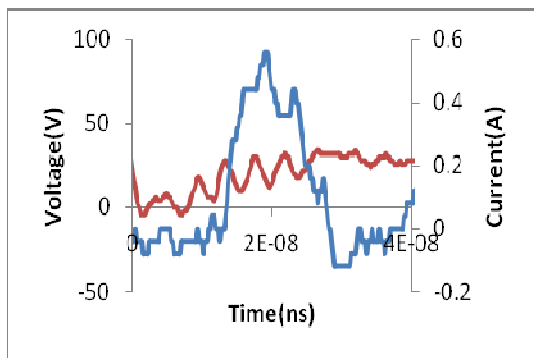
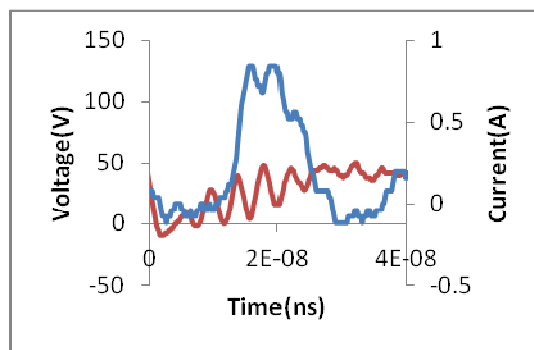
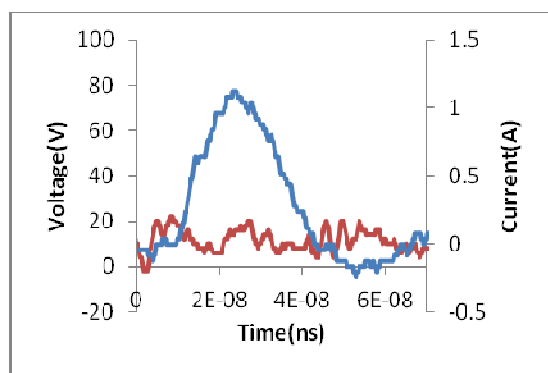
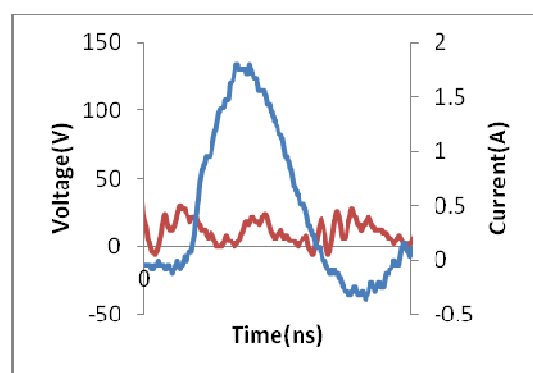
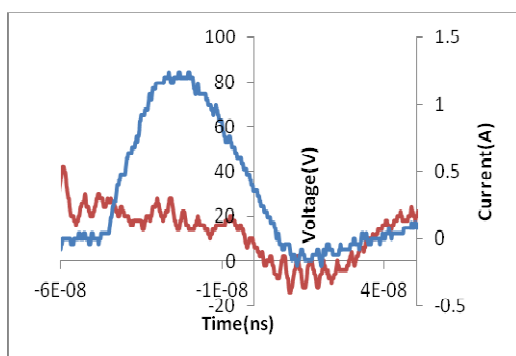
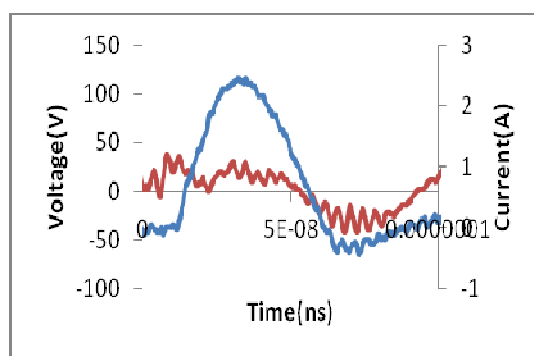
In this section, the process parameters measured from discharge current and voltage waveforms during discharge condition is discussed. In addition, the effect of discharge energy and pulse on time on crater geometry is also discussed.

5.3.1 Measurement of Process Parameters

The typical voltage and current waveforms recorded on oscilloscope during each single pulse discharge condition from I to VI are shown in Figure 5.2. From each of the waveform captured, electrical discharge information's such as average voltage, average current and pulse on time were calculated using the equations mentioned in section 3.4.1. These average voltage and average current values during sparking can be calculated only over the portion of pulse on time durations. These values are used to calculate the fraction of energy input, defined as measured discharge energy during sparking. The calculated average voltage, average current and measured energy are shown in table 5.3

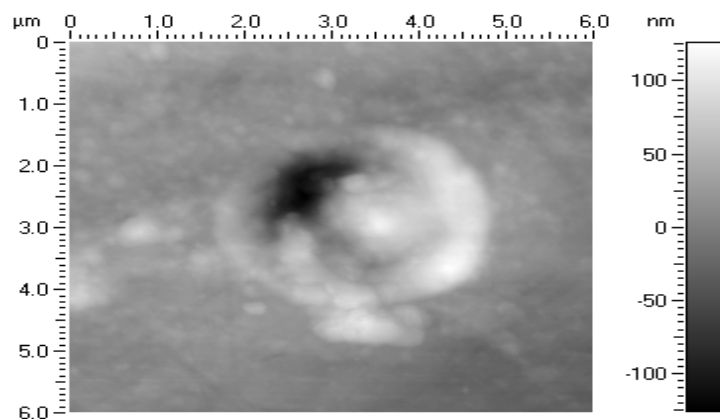
Table 5.3 Parameter measured from voltage and current waveform

Discharge Condition	Average Discharge Voltage [V]	Average Discharge Current [V]	Pulse on time [ns]	Measured discharge Energy [J]
Q1 V_{oc} 70	24.01	0.34	14.32	0.1
Q1 V_{oc} 110	31.22	0.57	14.8	0.238
Q2 V_{oc} 70	9.32	0.74	33.16	0.273
Q2 V_{oc} 110	12.02	1.03	36.96	0.373
Q3 V_{oc} 70	11.33	0.95	46.7	0.6
Q3 V_{oc} 110	13	1.51	49	1.087

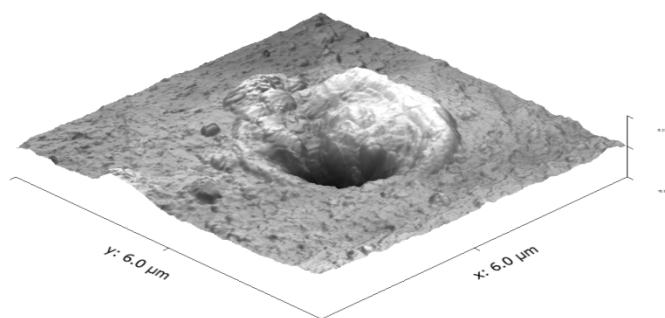
(a) Discharge condition I (0.1 μJ)(b) Discharge condition II (0.238 μJ)(c) Discharge condition III (0.273 μJ)(d) Discharge condition IV (0.373 μJ)(e) Discharge condition V (0.6 μJ)(f) Discharge condition VI (1.087 μJ)**Figure 5.2** Waveform at various discharge conditions

The size and shape of craters generated under different discharge conditions is measured using the Nanoscope IIIa-phase atomic force microscope (AFM). AFM uses J-type scanner head at tapping mode, scanning rate and resolution. This measured crater size for different discharge conditions is compared with predicted model.

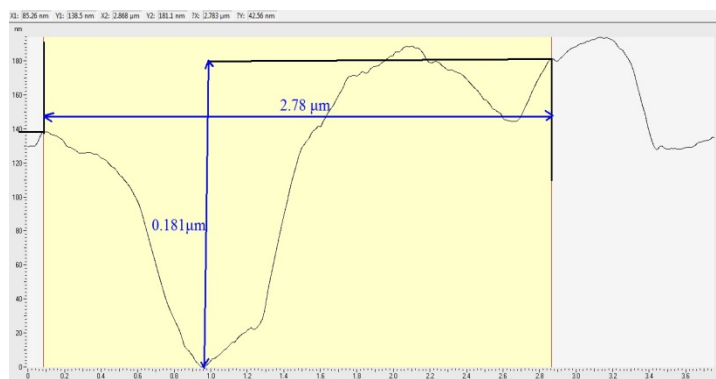
The AFM height map, AFM 3D image and cross-section of craters generated under micro-EDM discharge conditions from I to VI is shown in Figure 5.3 to Figure 5.8 respectively. The visual assessment of crater morphology produced under different discharge condition can be done using AFM height map and AFM 3D image. The crater cross section profile which is obtained from AFM data is used to measure crater diameter and depth.



(a) AFM height map

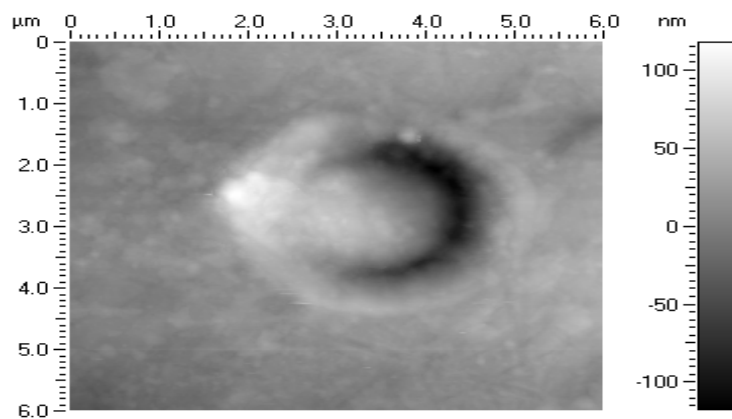


(b) AFM 3D image

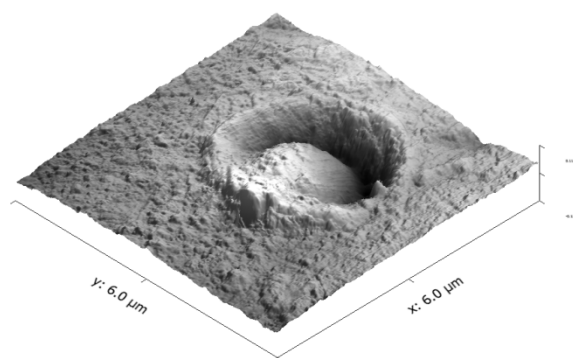


(c) Cross sectional of profile

Figure 5.3 Experimental crater formed under Discharge condition I ($0.1 \mu\text{J}$)



(a) AFM height map

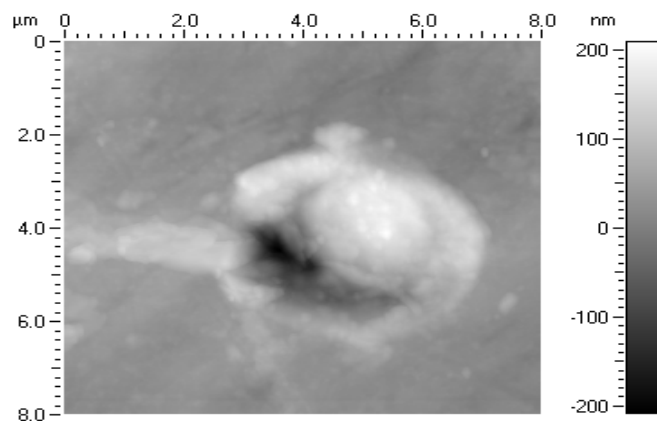


(b) AFM 3D image

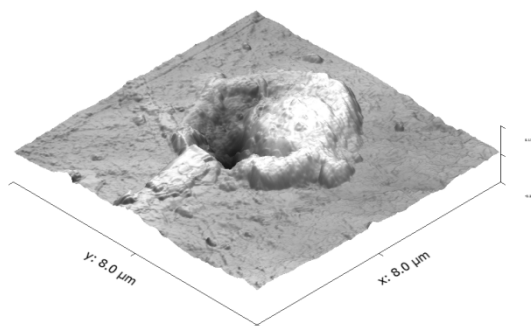


(c) Cross sectional profile

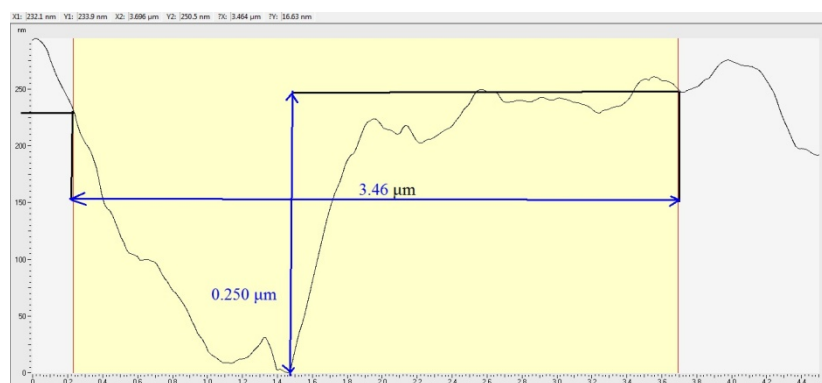
Figure 5.4 Experimental crater formed under Discharge condition II (0.238 μJ)



(a) AFM height map

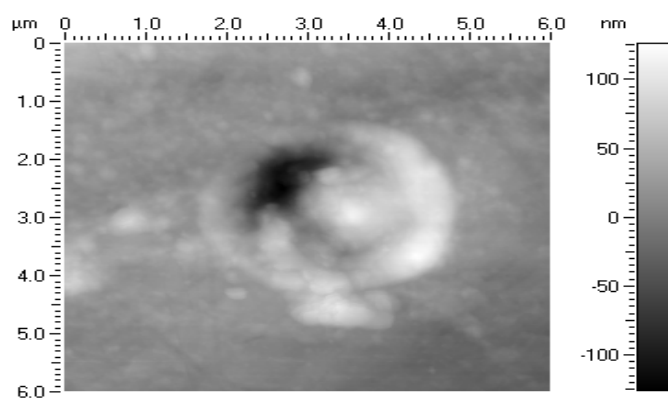


(b) AFM 3D image

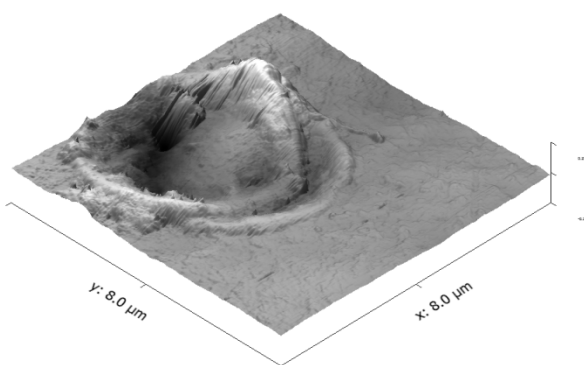


(c) Cross sectional profile

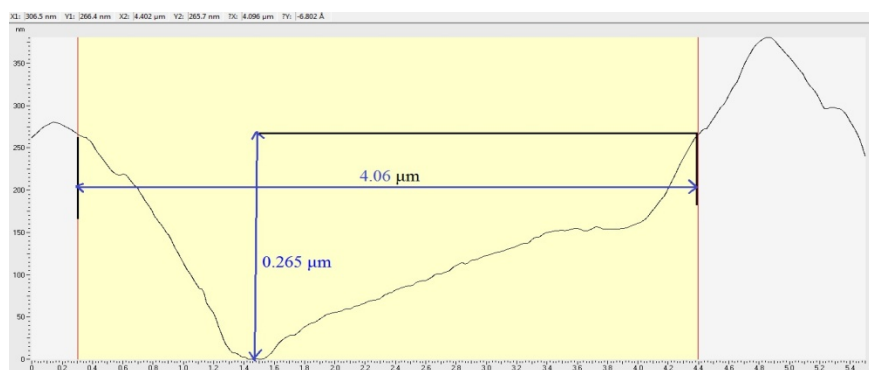
Figure 5.5 Experimental crater formed under Discharge condition III (0.273 μJ)



AFM height map

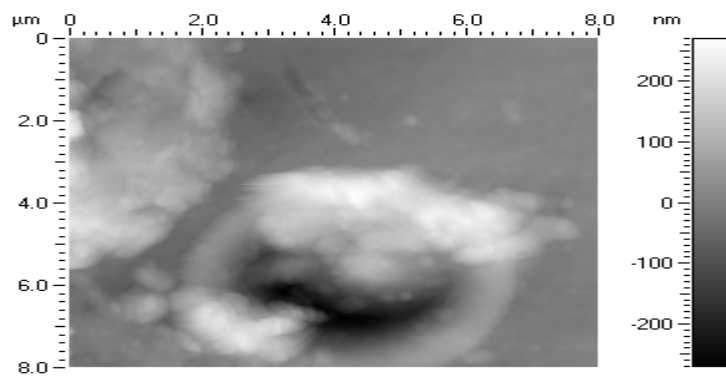


AFM 3D image

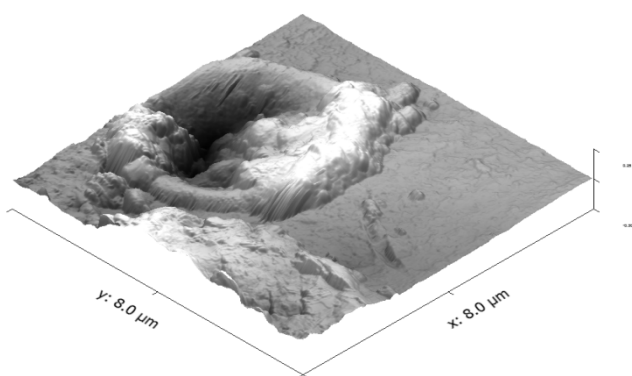


Cross sectional profile

Figure 5.6 Experimental crater formed under Discharge condition IV (0.373 μJ)



AFM height map

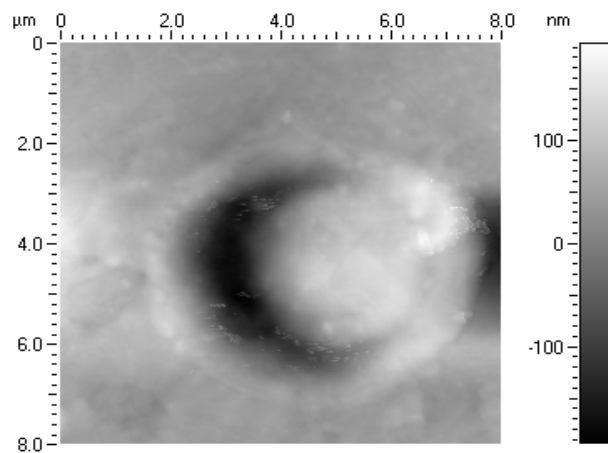


AFM 3D image

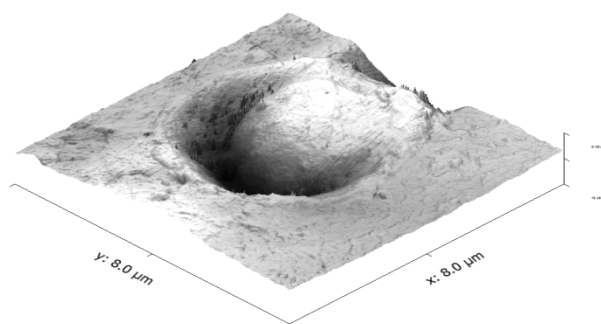


Cross sectional profile

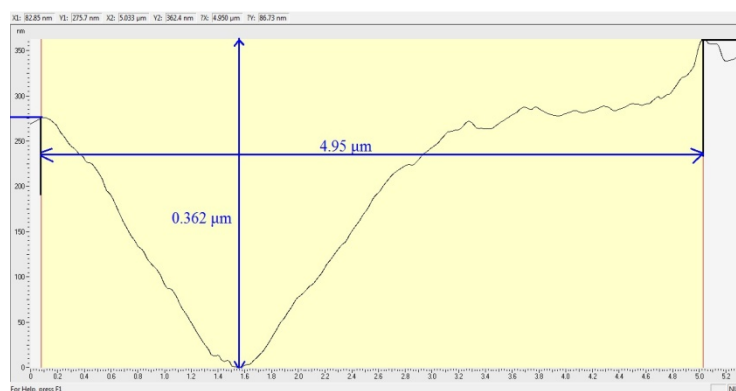
Figure 5.7 Experimental crater formed under Discharge condition V (0.6 μJ)



AFM height map



AFM 3D image



Cross sectional profile

Figure 5.8 Experimental crater formed under Discharge condition VI (1.087 μJ)

As shown in Figure 5.3 to Figure 5.8, all the craters produced with a depressed center for discharge condition from I to IV. This crater morphology may be created by superheating of molten material within the crater due to the high pressure of plasma channel [58][103].

5.3.2 Effect of discharge Energy on crater Geometry

As seen from cross sectional profile of crater (also from Figure 5.9 and 5.10) for discharge condition I to VI, the crater diameter and crater depth increases with increase in measured discharge energy. When the discharge energy is 0.1, 0.238, 0.273, .0.373, 0.6 μJ , crater radius is 1.39, 1.59, 1.73, 2.2, 2.48 μm and peak crater depth is around 0.181, 0.192, 0.25, 0.27, 0.33, 0.36 μm .

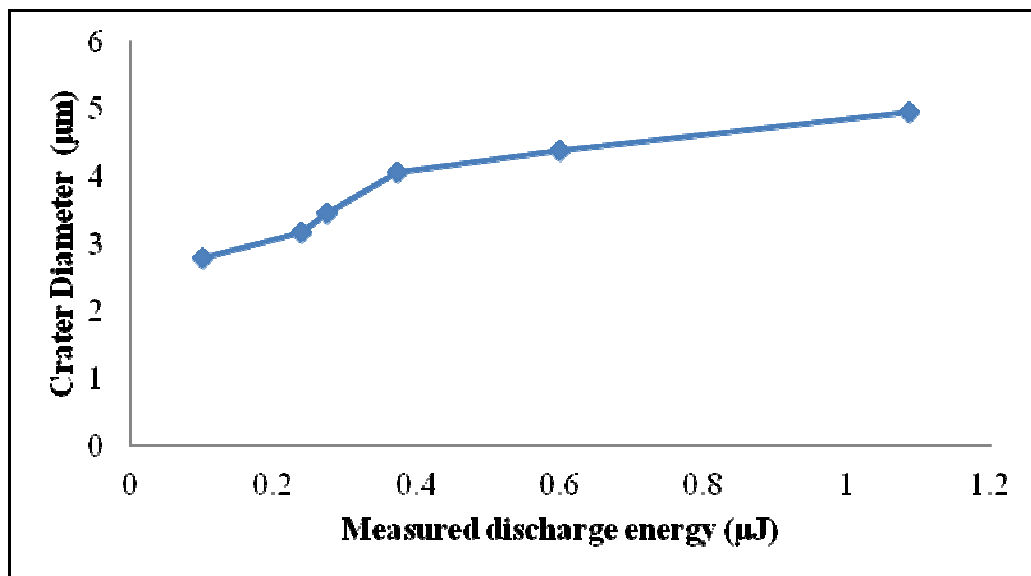


Figure 5.9 Effect of measured discharge energy on crater diameter

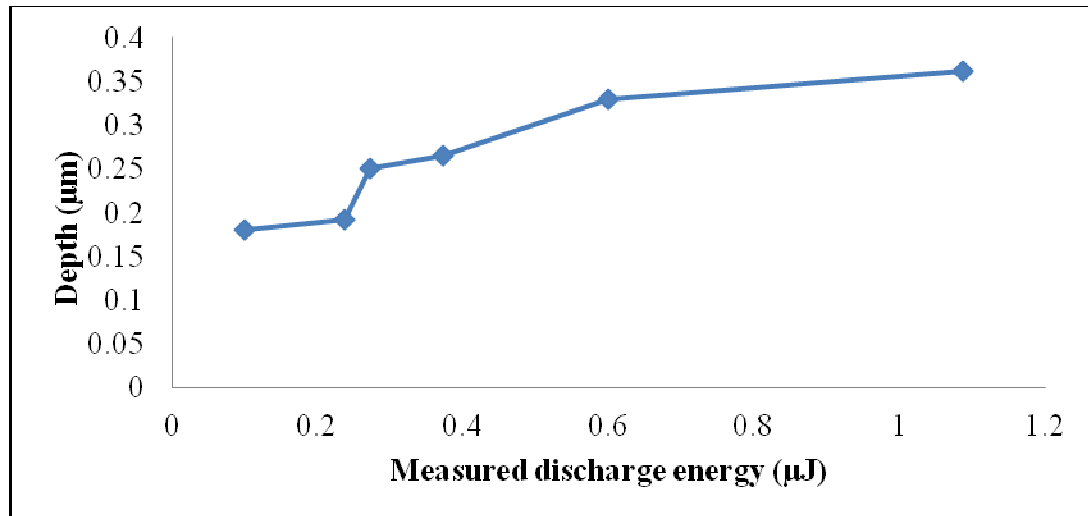


Figure 5.10 Effect of measured discharge energy on crater depth

5.3.3 Effect of Pulse on time on crater geometry

Figure 5.11 and 5.12 show the effect of pulse on time on crater radius and crater depth respectively. Crater diameter and crater depth increases with increase in pulse on time.

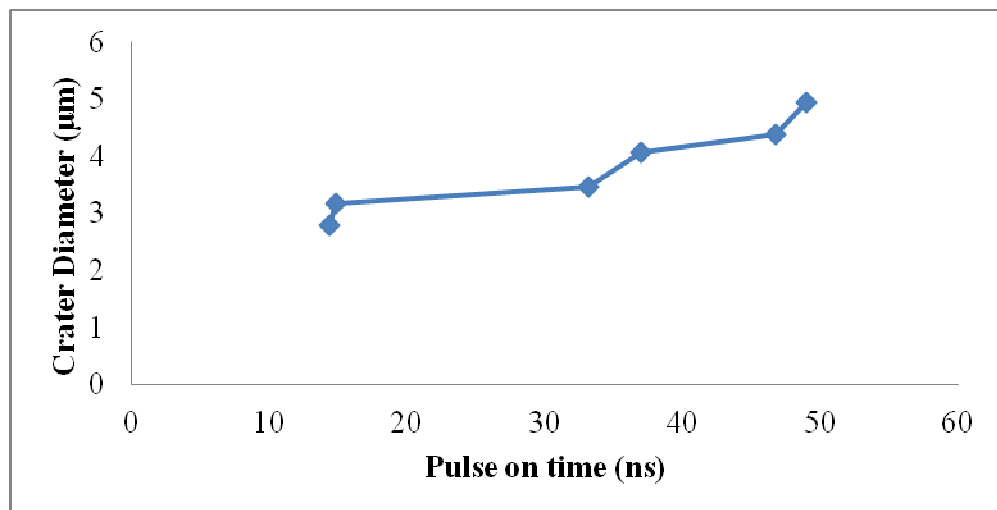


Figure 5.11 Effect of Pulse on time on Crater Diameter

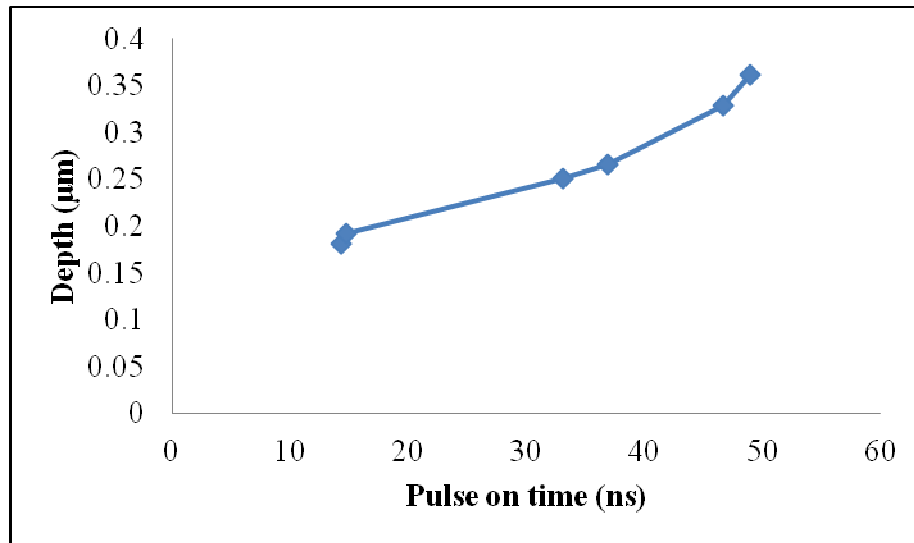
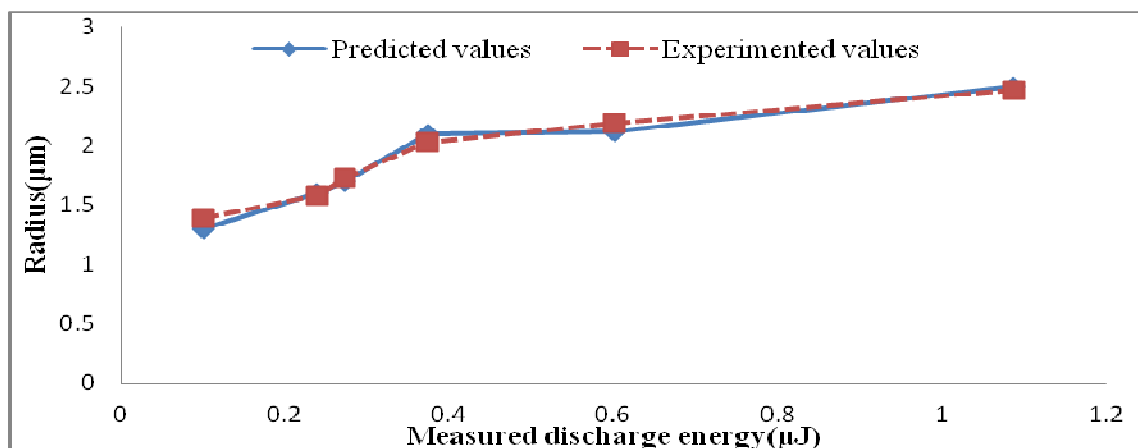


Figure 5.12 Effect of Pulse on time on Crater Depth

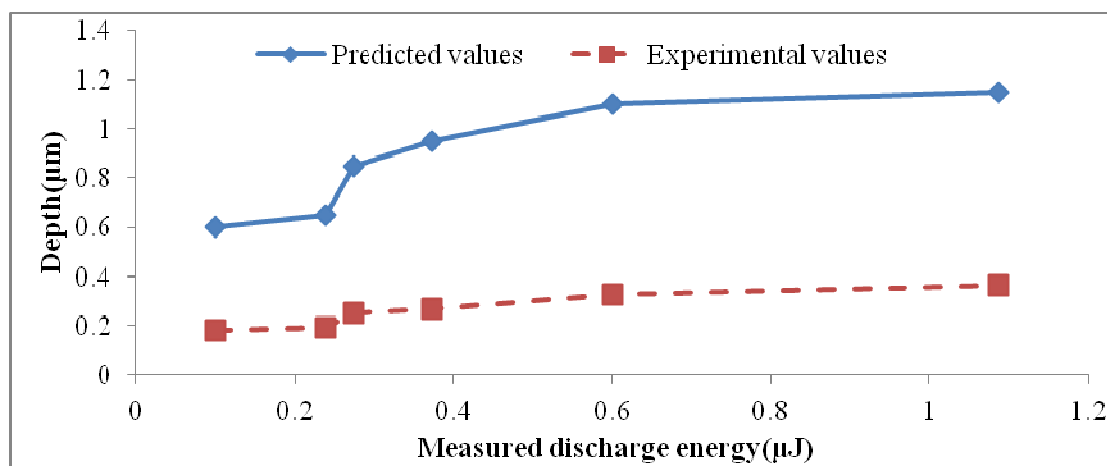
5.4 Model Verification

In this section predictive results of model obtained through simulation in previous chapter were compared with the experimental data. Table 5.3 presents the machining conditions. The model was verified for different discharge energy.

Figure 5.12 (a) and 5.12 (b) shows the comparison of simulated radius and depth values with experimental crater radius and depth values. The model estimates crater radius values within the range of measured values for all experiments. However, model overestimates crater depth values for all experimental discharge conditions considered. This overestimates in crater depth values might be due to the inability of collapsing plasma channel to eject all the molten material.



(a) Crater radius



(b) Crater depth

Figure 5.13 Comparison of predicted and experimental crater geometries

CHAPTER 6

CONCLUSIONS AND RECOMMENDATIONS

6.1 Conclusions

A predictive model based on heat transfer principles was developed for estimating the crater geometry during single spark machining for micro-EDM process. This model is solved by finite element method. This model used a Gaussian distribution of heat source, constant plasma radius and is equal to measured crater size, temperature dependant material properties to perform transient thermal analysis in order to predict crater geometry, temperature distribution on the workpiece at different energy level. This model assumed that the material was removed when its temperature exceeds the melting temperature during pulse on time. Experimental crater geometries measured by atomic force microscope (AFM) were compared with the simulation crater geometries.

1. Crater radius and crater depth are proportional to discharge energy level.
2. In temperature distribution simulation, there is rapid increase in temperature on the workpiece surface as compared to workpiece beneath the top surface. Also the maximum temperature in simulation is higher than melting temperature which supports the assumption that the certain part is removed whose temperature is higher than melting temperature.

3. As the simulated crater radius values for different discharge energy level (less than μJ) were found to be in agreement with measured experimental values. The assumptions made in this simulation approach such as constant plasma radius and is equal to measured crater radius, Gaussian distribution of heat source and fraction of total energy transferred to workpiece were proved to be reasonable.
4. Simulation results overestimates crater depth value for different discharge energy level due to the inability of collapsing plasma channel to eject all the molten material.

6.2 Recommendations for future work

1. This model is highly dependent on the empirical value of crater radius. Further experimental study should be done in order to approximate time dependant plasma radius over wider discharge energy input range.
2. Incorporating the time dependant plasma radius, effect of plasma pressure and enthalpy of material will give better simulation model in understanding the crater formation for a single discharge micro-EDM.
3. Further work can be done by extending the single discharge theory and incorporating a plasma flushing efficiency to simulate multi sparking phenomena in micro-EDM. This will give better prediction of performance measures such as crater geometry, surface roughness and recast layer thickness and also more appropriate description of process mechanism in micro-EDM.

REFERENCES

1. Dimov, S., et al. A roadmapping study in multi-material micro manufacture. in Proceedings of Second International Conference on Multi-Material Micro Manufacture. 2006.
2. Craven, D. Photolithography challenges for the micromachining industry. in 16th Annual BACUS Symposium on Photomask Technology and Management. 1996. International Society for Optics and Photonics.
3. Brousseau, E., S. Dimov, and D. Pham, Some recent advances in multi-material micro-and nano-manufacturing. The International Journal of Advanced Manufacturing Technology, 2010. **47**(1-4): p. 161-180.
4. Liu, X., et al., The mechanics of machining at the microscale: assessment of the current state of the science. Journal of manufacturing science and engineering, 2004. **126**(4): p. 666-678.
5. Dornfeld, D., S. Min, and Y. Takeuchi, Recent advances in mechanical micromachining. CIRP Annals-Manufacturing Technology, 2006. **55**(2): p. 745-768.
6. El-Hofy, H.A.-G., Advanced machining processes: nontraditional and hybrid machining processes. 2005: McGraw Hill Professional.
7. Li, X., J. Wang, and W. Li. Current state and prospect of micro-machining. in Automation and Logistics, 2007 IEEE International Conference on. 2007. IEEE.
8. Rajurkar, K., et al., Micro and nano machining by electro-physical and chemical processes. CIRP Annals-Manufacturing Technology, 2006. **55**(2): p. 643-666.
9. Pham, D.T., et al., Micro-EDM—recent developments and research issues. Journal of Materials Processing Technology, 2004. **149**(1): p. 50-57.
10. Ho, K. and S. Newman, State of the art electrical discharge machining (EDM). International Journal of Machine Tools and Manufacture, 2003. **43**(13): p. 1287-1300.
11. Sen, B., et al. Developments in electric power supply configurations for electrical-discharge-machining (EDM). in Power Electronics and Drive Systems, 2003. PEDS 2003. The Fifth International Conference on. 2003. IEEE.
12. Kunieda, M., et al., Advancing EDM through fundamental insight into the process. CIRP Annals-Manufacturing Technology, 2005. **54**(2): p. 64-87.
13. Han, F., S. Wachi, and M. Kunieda, Improvement of machining characteristics of micro-EDM using transistor type isopulse generator and servo feed control. Precision Engineering, 2004. **28**(4): p. 378-385.
14. Han, F., et al., Basic study on pulse generator for micro-EDM. The International Journal of Advanced Manufacturing Technology, 2007. **33**(5-6): p. 474-479.
15. Lee, H.-T. and J.-P. Yur, Characteristic analysis of EDMed surfaces using the Taguchi approach. Materials and Manufacturing Processes, 2000. **15**(6): p. 781-806.
16. Tariq Jilani, S. and P. Pandey, An analysis of surface erosion in electrical discharge machining. Wear, 1983. **84**(3): p. 275-284.
17. Pandit, S.M. and K.P. Rajurkar. Mathematical Model for Electro-Discharge Machined Surface Roughness. in 1978 SME Manufacturing Engineering Transactions and 6 th North American Metalworking Research Conference Proceedings. SME, Dearborn, Mich. 1978, 339-345. 1978.

18. Rajurkar, K. and S. Pandit, Quantitative Expressions for Some Aspects of Surface Integrity of Electrodischarge Machined Components. *J. Eng. Ind.(Trans. ASME)*, 1984. **106**(2): p. 171-177.
19. Lee, L., et al., Quantification of surface damage of tool steels after EDM. *International Journal of Machine Tools and Manufacture*, 1988. **28**(4): p. 359-372.
20. Weck, M. and J. Dehmer, Analysis and adaptive control of EDM sinking process using the ignition delay time and fall time as parameter. *CIRP Annals-Manufacturing Technology*, 1992. **41**(1): p. 243-246.
21. Rajurkar, K. and W. Wang, Improvement of EDM performance with advanced monitoring and control systems. *Journal of manufacturing science and engineering*, 1997. **119**(4): p. 770-775.
22. Dauw, D. and B. Van Coppenolle. On the evolution of EDM research Part 2: from fundamental research to applied research. in *Proceedings of the 11th International Symposium on Electromachining*. 1995.
23. Masuzawa, T., et al., Wire electro-discharge grinding for micro-machining. *CIRP Annals-Manufacturing Technology*, 1985. **34**(1): p. 431-434.
24. Masuzawa, T., J. Tsukamoto, and M. Fujino, Drilling of deep microholes by EDM. *CIRP Annals-Manufacturing Technology*, 1989. **38**(1): p. 195-198.
25. Mohri, N., et al., Assisting electrode method for machining insulating ceramics. *CIRP Annals-Manufacturing Technology*, 1996. **45**(1): p. 201-204.
26. Mohri, N., et al., Some considerations to machining characteristics of insulating ceramics-towards practical use in industry. *CIRP Annals-Manufacturing Technology*, 2002. **51**(1): p. 161-164.
27. Jeswani, M., Effect of the addition of graphite powder to kerosene used as the dielectric fluid in electrical discharge machining. *Wear*, 1981. **70**(2): p. 133-139.
28. Ming, Q.Y. and L.Y. He, Powder-suspension dielectric fluid for EDM. *Journal of materials processing technology*, 1995. **52**(1): p. 44-54.
29. Fleischer, J., J. Schmidt, and S. Haupt, Combination of electric discharge machining and laser ablation in microstructuring of hardened steels. *Microsystem technologies*, 2006. **12**(7): p. 697-701.
30. Zhixin, J., Z. Jianhua, and A. Xing, Study on a new kind of combined machining technology of ultrasonic machining and electrical discharge machining. *International Journal of Machine Tools and Manufacture*, 1997. **37**(2): p. 193-199.
31. Kunieda, M., M. Yoshida, and N. Taniguchi, Electrical discharge machining in gas. *CIRP Annals-Manufacturing Technology*, 1997. **46**(1): p. 143-146.
32. Kunieda, M., et al., High speed 3D milling by dry EDM. *CIRP Annals-Manufacturing Technology*, 2003. **52**(1): p. 147-150.
33. Kunieda, M., T. Takaya, and S. Nakano, Improvement of dry EDM characteristics using piezoelectric actuator. *CIRP Annals-Manufacturing Technology*, 2004. **53**(1): p. 183-186.
34. Joshi, S., et al., Experimental characterization of dry EDM performed in a pulsating magnetic field. *CIRP Annals-Manufacturing Technology*, 2011. **60**(1): p. 239-242.
35. Kao, C., J. Tao, and A.J. Shih, Near dry electrical discharge machining. *International Journal of Machine Tools and Manufacture*, 2007. **47**(15): p. 2273-2281.

36. Masaki, T., K. Kawata, and T. Masuzawa. Micro electro-discharge machining and its applications. in *Micro Electro Mechanical Systems, 1990. Proceedings, An Investigation of Micro Structures, Sensors, Actuators, Machines and Robots*. IEEE. 1990. IEEE.
37. König, W., et al., EDM-future steps towards the machining of ceramics. *CIRP Annals-Manufacturing Technology*, 1988. **37**(2): p. 623-631.
38. Yu, Z., K. Rajurkar, and H. Shen, High aspect ratio and complex shaped blind micro holes by micro EDM. *CIRP Annals-Manufacturing Technology*, 2002. **51**(1): p. 359-362.
39. Zhao, W., et al., A CAD/CAM system for micro-ED-milling of small 3D freeform cavity. *Journal of materials processing technology*, 2004. **149**(1): p. 573-578.
40. Yeo, S.H., et al., Processing of Zirconium-based bulk metallic glass (BMG) using micro electrical discharge machining (Micro-EDM). *Materials and Manufacturing Processes*, 2009. **24**(12): p. 1242-1248.
41. Cusanelli, G., et al. Properties of micro-holes for nozzle by micro-EDM. in *15th International Symposium on Electromachining (ISEM XV)*. 2007.
42. Masuzawa, T. and H. Tönshoff, Three-dimensional micromachining by machine tools. *CIRP Annals-Manufacturing Technology*, 1997. **46**(2): p. 621-628.
43. Muttamara, A., et al., Probability of precision micro-machining of insulating Si₃N₄ ceramics by EDM. *Journal of Materials Processing Technology*, 2003. **140**(1): p. 243-247.
44. Reynaerts, D., P.-H.s. Heeren, and H. Van Brussel, Microstructuring of silicon by electro-discharge machining (EDM)—part I: theory. *Sensors and Actuators A: Physical*, 1997. **60**(1): p. 212-218.
45. Kim, S., et al., Hybrid micromachining using a nanosecond pulsed laser and micro EDM. *Journal of micromechanics and microengineering*, 2010. **20**(1): p. 015037.
46. Yeo, S. and M. Murali, A new technique using foil electrodes for the electro-discharge machining of micro grooves. *Journal of Micromechanics and Microengineering*, 2003. **13**(1): p. N1.
47. Jahan, M., Y. Wong, and M. Rahman, A study on the quality micro-hole machining of tungsten carbide by micro-EDM process using transistor and RC-type pulse generator. *Journal of Materials Processing Technology*, 2009. **209**(4): p. 1706-1716.
48. Hang, G., et al. Micro-EDM milling of micro platinum hemisphere. in *Nano/Micro Engineered and Molecular Systems, 2006. NEMS'06. 1st IEEE International Conference on*. 2006. IEEE.
49. Schoth, A., R. Förster, and W. Menz, Micro wire EDM for high aspect ratio 3D microstructuring of ceramics and metals. *Microsystem technologies*, 2005. **11**(4-5): p. 250-253.
50. Masuzawa, T., et al., EDM-lathe for micromachining. *CIRP Annals-Manufacturing Technology*, 2002. **51**(1): p. 355-358.
51. Schumacher, B.M., After 60 years of EDM the discharge process remains still disputed. *Journal of Materials Processing Technology*, 2004. **149**(1): p. 376-381.

52. Dhanik, S., et al., Evolution of EDM process modelling and development towards modelling of the micro-EDM process. *International journal of manufacturing technology and management*, 2005. **7**(2): p. 157-180.
53. Eubank, P.T., et al., Theoretical models of the electrical discharge machining process. III. The variable mass, cylindrical plasma model. *Journal of applied physics*, 1993. **73**(11): p. 7900-7909.
54. Singh, A. and A. Ghosh, A thermo-electric model of material removal during electric discharge machining. *International Journal of Machine Tools and Manufacture*, 1999. **39**(4): p. 669-682.
55. Natsu, W., et al., Temperature distribution measurement in EDM arc plasma using spectroscopy. *JSME International Journal Series C*, 2004. **47**(1): p. 384-390.
56. Albinski, K., et al., The temperature of a plasma used in electrical discharge machining. *Plasma Sources Science and Technology*, 1996. **5**(4): p. 736.
57. Dhanik, S. and S.S. Joshi, Modelling of a single resistance capacitance pulse discharge in micro-electro discharge machining. *Journal of manufacturing science and engineering*, 2005. **127**(4): p. 759-767.
58. Pandey, P. and S. Jilani, Plasma channel growth and the resolidified layer in EDM. *Precision Engineering*, 1986. **8**(2): p. 104-110.
59. DiBitonto, D.D., et al., Theoretical models of the electrical discharge machining process. I. A simple cathode erosion model. *Journal of Applied Physics*, 1989. **66**(9): p. 4095-4103.
60. Jeswani, M., Electrical discharge machining in distilled water. *Wear*, 1981. **72**(1): p. 81-88.
61. Yan, B.H., H. Chung Tsai, and F. Yuan Huang, The effect in EDM of a dielectric of a urea solution in water on modifying the surface of titanium. *International Journal of Machine Tools and Manufacture*, 2005. **45**(2): p. 194-200.
62. Lonardo, P. and A. Bruzzone, Effect of flushing and electrode material on die sinking EDM. *CIRP Annals-Manufacturing Technology*, 1999. **48**(1): p. 123-126.
63. Masuzawa, T., X. Cui, and N. Taniguchi, Improved jet flushing for EDM. *CIRP Annals-Manufacturing Technology*, 1992. **41**(1): p. 239-242.
64. Guu, Y. and H. Hocheng, Effects of workpiece rotation on machinability during electrical-discharge machining. *Materials and Manufacturing Processes*, 2001. **16**(1): p. 91-101.
65. Huang, H., et al., Ultrasonic vibration assisted electro-discharge machining of microholes in Nitinol. *Journal of micromechanics and microengineering*, 2003. **13**(5): p. 693.
66. Yeo, S., M. Murali, and H. Cheah, Magnetic field assisted micro electro-discharge machining. *Journal of Micromechanics and Microengineering*, 2004. **14**(11): p. 1526.
67. Murali, M. and S. Yeo, A novel spark erosion technique for the fabrication of high aspect ratio micro-grooves. *Microsystem technologies*, 2004. **10**(8-9): p. 628-632.
68. Guu, Y., et al., Effect of electrical discharge machining on surface characteristics and machining damage of AISI D2 tool steel. *Materials Science and Engineering: A*, 2003. **358**(1): p. 37-43.

69. Lee, H.-T. and T.-Y. Tai, Relationship between EDM parameters and surface crack formation. *Journal of Materials Processing Technology*, 2003. **142**(3): p. 676-683.
70. Ramakrishnan, R. and L. Karunamoorthy, Modelling and multi-response optimization of Inconel 718 on machining of CNC WEDM process. *Journal of materials processing technology*, 2008. **207**(1): p. 343-349.
71. Sarkar, S., S. Mitra, and B. Bhattacharyya, Parametric analysis and optimization of wire electrical discharge machining of γ -titanium aluminide alloy. *Journal of Materials Processing Technology*, 2005. **159**(3): p. 286-294.
72. Chiang, K.-T. and F.-P. Chang, Applying grey forecasting method for fitting and predicting the performance characteristics of an electro-conductive ceramic (Al₂O₃+ 30% TiC) during electrical discharge machining. *The International Journal of Advanced Manufacturing Technology*, 2007. **33**(5-6): p. 480-488.
73. Petropoulos, G., N. Vaxevanidis, and C. Pandazaras, Modelling of surface finish in electro-discharge machining based upon statistical multi-parameter analysis. *Journal of Materials Processing Technology*, 2004. **155**: p. 1247-1251.
74. Habib, S.S., Study of the parameters in electrical discharge machining through response surface methodology approach. *Applied Mathematical Modelling*, 2009. **33**(12): p. 4397-4407.
75. Pradhan, M., R. Das, and C. Biswas, Comparisons of neural network models on surface roughness in electrical discharge machining. *Proceedings of the Institution of Mechanical Engineers, Part B: Journal of Engineering Manufacture*, 2009. **223**(7): p. 801-808.
76. Snoeys, R. and F. Van Dijck, Investigation of electro discharge machining operations by means of thermo-mathematical model. *CIRP Ann*, 1971. **20**(1): p. 35-37.
77. Van Dijck, F. and W. Dutre, Heat conduction model for the calculation of the volume of molten metal in electric discharges. *Journal of Physics D: Applied Physics*, 1974. **7**(6): p. 899.
78. Yeo, S., W. Kurnia, and P. Tan, Critical assessment and numerical comparison of electro-thermal models in EDM. *Journal of materials processing technology*, 2008. **203**(1): p. 241-251.
79. Beck, J.V., Transient temperatures in a semi-infinite cylinder heated by a disk heat source. *International Journal of Heat and Mass Transfer*, 1981. **24**(10): p. 1631-1640.
80. Beck, J.V., Large time solutions for temperatures in a semi-infinite body with a disk heat source. *International Journal of Heat and Mass Transfer*, 1981. **24**(1): p. 155-164.
81. Tariq Jilani, S. and P. Pandey, Analysis and modelling of EDM parameters. *Precision Engineering*, 1982. **4**(4): p. 215-221.
82. Pandit, S. and K. Rajurkar, A stochastic approach to thermal modelling applied to electro-discharge machining. *Journal of heat transfer*, 1983. **105**(3): p. 555-562.
83. Patel, M.R., et al., Theoretical models of the electrical discharge machining process. II. The anode erosion model. *Journal of Applied Physics*, 1989. **66**(9): p. 4104-4111.

84. Madhu, P., et al., Finite element analysis of EDM process. *Processing of Advanced Materials(UK)*, 1991. **1**(3): p. 161-173.
85. Das, S., M. Klotz, and F. Klocke, EDM simulation: finite element-based calculation of deformation, microstructure and residual stresses. *Journal of Materials Processing Technology*, 2003. **142**(2): p. 434-451.
86. Marafona, J. and J. Chousal, A finite element model of EDM based on the Joule effect. *International Journal of Machine Tools and Manufacture*, 2006. **46**(6): p. 595-602.
87. Joshi, S. and S. Pande, Thermo-physical modelling of die-sinking EDM process. *Journal of Manufacturing Processes*, 2010. **12**(1): p. 45-56.
88. Murali, M.S. and S.-H. Yeo, Process simulation and residual stress estimation of micro-electrodischarge machining using finite element method. *Japanese journal of applied physics*, 2005. **44**: p. 5254.
89. Allen, P. and X. Chen, Process simulation of micro electro-discharge machining on molybdenum. *Journal of materials processing technology*, 2007. **186**(1): p. 346-355.
90. Yeo, S., W. Kurnia, and P. Tan, Electro-thermal modelling of anode and cathode in micro-EDM. *Journal of Physics D: Applied Physics*, 2007. **40**(8): p. 2513.
91. Tan, P. and S. Yeo, Modelling of overlapping craters in micro-electrical discharge machining. *Journal of Physics D: Applied Physics*, 2008. **41**(20): p. 205302.
92. Boothroyd, G. and W.A. Knight, *Fundamentals of metal machining and machine tools*. Vol. 198. 2005: CRC.
93. Schulze, H.P., et al., Comparison of measured and simulated crater morphology for EDM. *Journal of materials processing technology*, 2004. **149**(1): p. 316-322.
94. Singh, H., Experimental study of distribution of energy during EDM process for utilization in thermal models. *International Journal of Heat and Mass Transfer*, 2012.
95. Erden, A., F. Arinc, and M. Kögmen, Comparison of mathematical models for electric discharge machining. *Journal of Materials Processing and Manufacturing Science*, 1995. **4**: p. 163-176.
96. Yadav, V., V.K. Jain, and P.M. Dixit, Thermal stresses due to electrical discharge machining. *International Journal of Machine Tools and Manufacture*, 2002. **42**(8): p. 877-888.
97. Snoeys, R., F. Van Dijck, and J. Peters, Plasma channel diameter growth affects stock removal in EDM. *Annals of the CIRP*, 1972. **21**(1): p. 39-40.
98. Erden, A., Effect of materials on the mechanism of electric discharge machining(E. D. M.). *ASME, Transactions, Journal of Engineering Materials and Technology*, 1983. **105**: p. 132-138.
99. Khan, A.A., Role of Heat Transfer on Process Characteristics During Electrical Discharge Machining. *Developments in Heat Transfer*, 2009: p. 417-435.
100. Murali, M.S. and S.H. Yeo, Process simulation and residual stress estimation of micro-electrodischarge machining using finite element method. *Japanese journal of applied physics*, 2005. **44**: p. 5254.
101. Basak, I. and A. Ghosh, Mechanism of spark generation during electrochemical discharge machining: a theoretical model and experimental verification. *Journal of materials processing technology*, 1996. **62**(1): p. 46-53.

102. Zahiruddin, M. and M. Kunieda, Comparison of energy and removal efficiencies between micro and macro EDM. *CIRP Annals-Manufacturing Technology*, 2012.